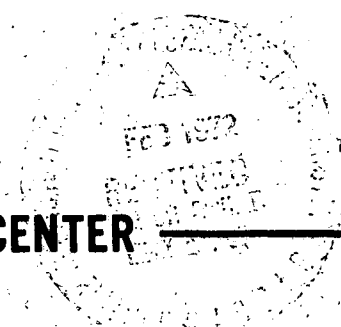


NASA TM X-65805

# SHOCK-METAMORPHIC EFFECTS IN THE LUNA-16 SOIL SAMPLE FROM MARE FECUNDITATIS

BEVAN M. FRENCH

NOVEMBER 1971



(NASA-TM-X-65805) SHOCK-METAMORPHIC EFFECTS IN THE LUNA-16 SOIL SAMPLE FROM MARE FECUNDITATIS B.M. French (NASA) Nov. CSCL 03B

**GODDARD SPACE FLIGHT CENTER  
GREENBELT, MARYLAND**

1971 50 p

N72-17908

FACILITY FORM

(PAU- G3/30  
TMX 650w  
(NASA CR OR TMX OR AD NUMBER)

Unclas  
17031

F

X-644-71-471

SHOCK-METAMORPHIC EFFECTS IN THE LUNA-16 SOIL SAMPLE  
FROM MARE FECUNDITATIS

Bevan M. French  
Planetology Branch

**Details of illustrations in  
this document may be better  
studied on microfiche**

November 1971

GODDARD SPACE FLIGHT CENTER  
Greenbelt, Maryland

SHOCK-METAMORPHIC EFFECTS IN THE LUNA-16 SOIL SAMPLE  
FROM MARE FECUNDITATIS

Bevan M. French  
Planetology Branch

ABSTRACT

Shock-metamorphic effects characteristic of meteorite impact and virtually identical to those observed in Apollo samples are common in fragments of the Luna-16 soil sample from Mare Fecunditatis. Two types of shock effects are present: (1) deformation and partial melting features in rock and mineral fragments (1-2 percent of fragments); (2) heterogeneous glasses and glassy breccias produced by shock melting (70-80 percent of fragments). Shock effects were observed in pyroxene (deformation twin lamellae; multiple planar shock lamellae; extreme mosaicism; partial isotropization); in plagioclase (planar shock lamellae; complete isotropization to form maskelynite); and in basalt fragments (plagioclase isotropization; selective partial melting). The glasses exhibit several characteristics of shock melting, especially: (1) diversity in chemical composition; (2) association with shocked mineral fragments and Ni-Fe spherules; (3) heterogeneous schlieren and incipient fusion of mineral inclusions.

Two types of source rocks are present in the Luna-16 sample, basaltic (85-90 percent) and feldspathic (gabbros to anorthosites) (10-15 percent). The basaltic rocks are predominant and generally occur as unshocked fragments, indicating that they form the bedrock underlying Mare Fecunditatis. The more shocked feldspathic material may have been transported from adjacent highlands or from nearby large postmare craters. The shock-metamorphic effects in the Luna-16 soil and its similarity to Apollo material indicate that regolith formation by meteorite impact has occurred on Mare Fecunditatis and is a general process over the entire moon.

CONTENTS

|  | <u>Page</u> |
|--|-------------|
| ABSTRACT . . . . .                           | iii         |
| INTRODUCTION . . . . .                       | 1           |
| METHODS OF STUDY . . . . .                   | 1           |
| COMPOSITION OF THE LUNAR SOIL . . . . .      | 2           |
| SHOCK-METAMORPHIC EFFECTS . . . . .          | 7           |
| Introduction . . . . .                       | 7           |
| Shocked Rock and Mineral Fragments . . . . . | 14          |
| Impact-Produced Glasses . . . . .            | 23          |
| CONCLUSIONS . . . . .                        | 38          |
| ACKNOWLEDGEMENTS . . . . .                   | 44          |
| REFERENCES . . . . .                         | 45          |

TABLES

| <u>Table</u>   | <u>Page</u> |
|--|-------------|
| 1 Abundances of Different Fragment Types in the Luna-16 Soil<br>Sample (Percent by number) . . . . . | 3           |
| 2 Electron Microprobe Analyses of Luna-16 Materials . . . . .  | 15          |

# SHOCK-METAMORPHIC EFFECTS IN THE LUNA-16 SOIL SAMPLE FROM MARE FECUNDITATIS

## INTRODUCTION

Intensive studies of returned lunar samples have confirmed the theory that the bedrock on lunar maria is overlain by a fragmental layer (regolith) of varying thickness which has been produced by continuing meteorite bombardment (1). The major evidence for this conclusion is the occurrence of distinctive shock-metamorphic effects, uniquely indicative of meteorite impact, in returned samples of fragmental lunar material. Virtually identical suites of shock features, including unique mineral deformation structures and unusual heterogeneous glasses, have been observed in samples from the Apollo 11 (2-7), Apollo 12 (8-11), and Apollo 14 (12) missions.

The Russian Luna-16 automated probe landed on Mare Fecunditatis on Sept. 20, 1970 and returned with 101 gm of fine-fragmental material obtained by drilling 35 cm into the regolith. Preliminary examination of the sample (13) showed that it consisted of diverse fragments generally about 0.1 mm in size, including both basaltic and anorthositic rock fragments, "cindery" and "slaggy" aggregates of glass and rock fragments, and glass fragments and free-form glasses similar to material obtained from the Apollo 11 and 12 missions. The Luna-16 sample is relatively low in  $\text{TiO}_2$  (13) and is thus chemically more similar to Apollo 12 material.

The purpose of this study was to examine the fragments for evidence of shock metamorphism in order to evaluate the role of meteorite impact in forming the lunar regolith at a new site relatively distant from the Apollo landing sites. The study was carried out as part of a consortium for mineralogy and petrology headed by J. A. Wood, Smithsonian Astrophysical Observatory (SAO). A shorter version of this paper has appeared in Earth and Planetary Science Letters (Special Luna-16 issue, vol. 13, no. 2, pp. 316-322, January, 1972).

## METHODS OF STUDY

The samples were obtained from SAO as fragments mounted on individually numbered polished thin sections, accompanied by index photographs giving each fragment a specific number (e.g., SAO 301,16). In the time available, four sections (301, 303, 315, and 318) were examined in detail, covering about 1000 fragments generally ranging in size from 50 to 200  $\mu\text{m}$ . The total weight of material studied was thus about 5-10 mg, and the importance of petrographic methods in studying shock effects is strongly emphasized by the fact that significant results were obtained nondestructively on such a small amount of material.

The samples were studied by conventional flat-stage petrographic microscopy in both transmitted and reflected light. A small number of electron microprobe analyses were made to verify visual mineral identifications and to investigate the chemical diversity of the glass fragments which is an indication of impact melting (e.g., 7). The probe analyses were made with an ARL/EMX instrument, using spectrometer detectors and analyzing for three elements at a time (Ca, Si, Mg/Fe, Ti, Al). The standards used were synthetic glasses kindly provided by F. R. Boyd, Geophysical Laboratory (14). The data were reduced by a modified Bence-Albee computer program (15).

## COMPOSITION OF THE LUNAR SOIL

The fragmental layer on Mare Fecunditatis, like that at the Apollo 11 and 12 sites, is composed of rock and mineral fragments, dense varicolored glass particles (both homogeneous and heterogeneous), and particles composed of mixtures of glass and rock fragments (13). The latter fragments are most common (Table 1) and are designated as microbreccias.\* They consist of small diverse rock, mineral, and glass fragments in a variable glass-bearing matrix. Three textural types of matrix can be distinguished in the Luna-16 material (Table 1), but the types are gradational and one fragment may often exhibit two or more different textures in the matrix. The fragments are very similar in character and abundance to those observed in Apollo material (17, 18).

---

\* The nomenclature of lunar soil particles is somewhat complicated, and a wide variety of terms has been used by other workers (13, 16-21) to describe virtually identical particles. In this study, microbreccia is a general term designating all fragments which are themselves composed of various small individual clasts of rocks, minerals, and glasses, contained in a matrix which may display a variety of textures ranging from finely-fragmental to completely glassy. The individual clasts may come from different sources and may record multiple events of brecciation and accretion.

The dark, probably basaltic microbreccias in the Luna-16 soil can be subdivided into three categories (Table 1) on the basis of the character of the matrix, and, to a lesser extent, on the ratio of fragments to matrix: (1) fine-fragmental matrix, composed of small angular clasts with little or no glass; (2) glassy/vesicular matrix, consisting of heterogeneous, flow-banded, generally vesicular glass which may contain Ni-Fe spherules; (3) welded/sintered matrix, which is dense and lacks both fine-fragmental texture and significant vesicularity. The textural types are gradational, and single fragments displaying two different textures are commonly observed.

The use of microbreccia as a general term to include all the particulate soil fragments is preferred because these particles evidently represent a continuum of textures, all reflecting impact-produced brecciation and melting. Furthermore, a subdivision based on recognizable textural differences seems preferable at the present time, particularly since there is considerable discussion about the origin of certain textures. Most of the glassy-vesicular fragments are probably the result of ballistic accretion of glass and rock fragments ejected from meteorite impact craters, but the fragmental-matrix and welded/sintered types may be produced by shock lithification (6) or by postdepositional welding of hot ejecta (18).

The terms used here can be closely related to those developed for the predominant, dark, and basaltic particles observed in other studies of Apollo 11, Apollo 12, and Luna-16 samples (13, 16-21). The fine-fragmental matrix breccias are equivalent to the "microbreccias" (19) or "soil breccias" (20). The glassy/vesicular matrix fragments correspond to the "microagglutinate particles" (16), "glazed aggregates" and "dark, inclusion-laden glass" (17), "cindery glasses" (18), "agglomerates and glass spatter" (19), and "cinders and slags" (13). The welded/sintered matrix fragments have not been separately distinguished by other workers, but they probably correspond to the "dense" or "coherent" "microbreccias" observed in the Apollo 11 soils (17-19) and in other samples.

A similar, though less detailed, subdivision based on matrix characteristics was also used for the lighter feldspathic microbreccias in the Luna-16 soil. Although such fragments are much less common, a sufficient number were observed to recognize two different types: (1) a glassy matrix variety, and (2) a crystalline or aphanitic matrix which may represent partly crystallized glass. The two types are approximately equivalent, respectively, to the Type B and Type C anorthosite fragments studied by Marvin and others in the Apollo 12 and Luna-16 soils (21, 24).

Table 1

**Abundances of Different Fragment Types in the Luna-16 Soil Sample  
(percent by number)**

| Section No.<br>Layer<br>Size<br>No. of Fragments                 | SAO 301<br>D<br>>250 $\mu\text{m}$<br>75 | SAO 303<br>D<br>>250 $\mu\text{m}$<br>65 | SAO 318<br>A<br>75-150 $\mu\text{m}$<br>579 | SAO 315<br>A<br>150-250 $\mu\text{m}$<br>236 |
|--|--|--|---|--|
| <b>I. Rock Fragments</b>   |  |  |   |  |
| A. Basaltic  | 13.3                                     | 20.0                                     | 19.2  | 21.2   |
| B. Feldspathic   | 4.0                                      | 1.5                                      | 2.4   | 1.3  |
| C. Individual crystals   |  |  |   |  |
| 1. plagioclase   | 1.3                                      | 0  | 1.2   | 0.4  |
| 2. pyroxene  | 0  | 0  | 4.8   | 0.4  |
| 3. olivine, others   | 0  | 0  | 2.2   | 1.3  |
| <b>II. Microbreccias</b>   |  |  |   |  |
| A. Dark (basaltic)   |  |  |   |  |
| 1. fine-fragmental matrix  | 8.0                                      | 9.2                                      | 7.8   | 8.9  |
| 2. glassy/vesicular matrix                                       | 38.7                                     | 26.1                                     | 22.1  | 40.7   |
| 3. welded/sintered matrix  | 17.3                                     | 12.3                                     | 23.5  | 8.5  |
| B. Light (feldspathic)   |  |  |   |  |
| 1. glassy matrix   | 2.7                                      | 3.1                                      | 0.5   | 2.1  |
| 2. crystalline or aphanitic matrix                               | 6.7                                      | 4.6                                      | 4.3   | 3.0  |
| <b>III. Glasses</b>  |  |  |   |  |
| A. Homogeneous, featureless<br>(including devitrified)           | 2.7                                      | 9.2                                      | 5.4   | 5.9  |
| B. Heterogeneous, flow-banded<br>(minor inclusions and vesicles) | 5.3                                      | 13.8                                     | 6.6   | 3.0  |
| <b>TOTAL</b>   | 100.0                                    | 99.8                                     | 100.0                                       | 100.1  |
| Basaltic (IA + IIA + III + IC2 + IC3)                            | 85.3                                     | 90.6                                     | 91.6  | 93.3   |
| Feldspathic (IB + IC1 + IIB)                                     | 14.7                                     | 9.2                                      | 8.4   | 6.8  |
| Shock-metamorphosed (II + III)                                   | 81.4                                     | 78.3                                     | 70.2  | 75.4   |
| Unshocked (I)  | 18.6                                     | 21.5                                     | 29.8  | 24.6   |

Two families of rock fragments have been recognized in the Luna-16 material (13). In this study, they are divided into basaltic rocks (with a variety of textures) and feldspathic rocks which range in composition from gabbros to anorthosites. Both families occur as rock and mineral fragments, as shocked rocks, and as diverse microbreccias composed of basaltic (dark) and feldspathic (light) components (Table 1). Composite fragments are often observed and generally consist of particles of light microbreccias included in dark microbreccia or glass.

Basaltic rocks are the most common. As unshocked and shocked rock fragments and as dark microbreccias, basaltic fragments constitute 85-90 percent of the fragments examined (Table 1). The basalts are generally unshocked and consist of clinopyroxene, plagioclase, and ilmenite, with minor olivine, spinel(?), Ni-Fe, and mesostasis (Figures 1-4). As far as can be estimated from the small fragments studied, opaque phases constitute less than 5-10 percent of the rocks, similar to the Apollo 12 basalts, a finding consistent with the relatively low TiO<sub>2</sub> content observed (13). The basaltic fragments show a variety of primary textures, including: (1) ophitic to subophitic (Figure 1); (2) microporphyritic, with larger (100 $\mu$ m) crystals of olivine in a fine groundmass (Figures 2, 3); (3) fine-grained to intersertal, often showing textures indicative of rapid quench crystallization from a melt (Figure 5).

Feldspathic rocks and their shocked and brecciated equivalents compose 10-15 percent of the fragments (Table 1). In contrast to the basalts, which commonly occur as unshocked rock fragments, the feldspathic rocks occur as rare, apparently shocked, fragments (Figures 5-8) and most commonly as light microbreccias with microgranular, microcrystalline, and glassy groundmasses (Figures 9-11). Many of the microbreccia fragments are clear, apparently plagioclase-rich, and often microgranular (Figure 9), resembling anorthositic particles observed in the Apollo 11 and Apollo 12 soils (e.g., 20, 21). Other microbreccia fragments are buff, yellow-brown, and brownish-gray in transmitted light (Figures 10, 11) and show some textural similarities to the unusual KREEP fragments from Apollo 12 (22, 23). However, preliminary analytical results (24) indicate that these fragments do not have the unusual high-K, high-P chemistry of KREEP fragments and are gabbroic to anorthositic in composition.

Light-colored microbreccia fragments are often found as inclusions in a matrix of dark microbreccia (Figure 12) or as cores surrounded by a rim of dark, probably basaltic, glass (Figure 13). However, fragments of dark (basaltic) microbreccia were not observed as inclusions in lighter-colored feldspathic rocks.

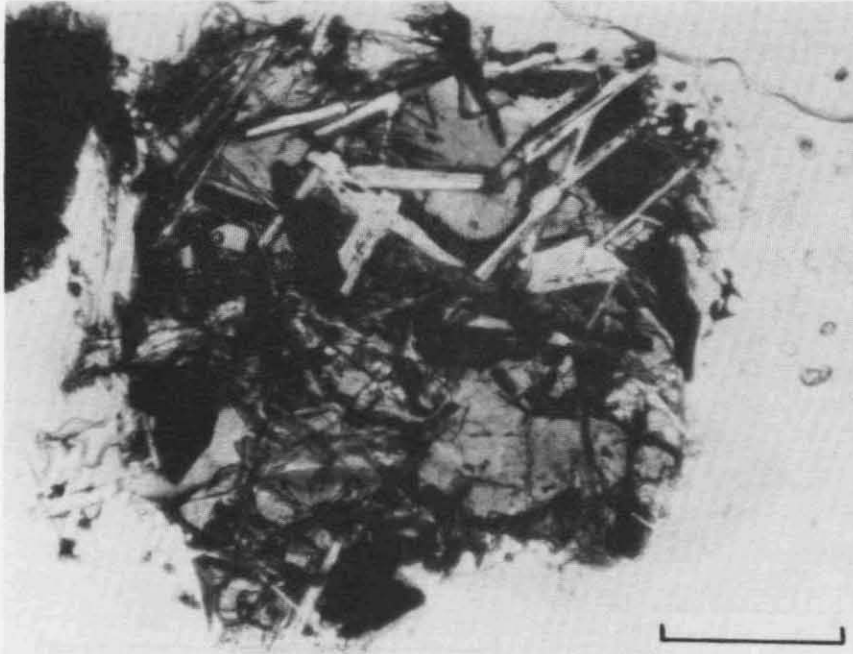


Figure 1. Fine-grained subophitic basalt fragment, composed of larger crystals of clinopyroxene (gray), with laths of plagioclase feldspar (white), and euhedral crystals of ilmenite (gray). A fine-grained intergranular mesostasis occurs in the central part of the specimen. Fragment 301,1; plane polarized light; scale bar 0.1 mm.

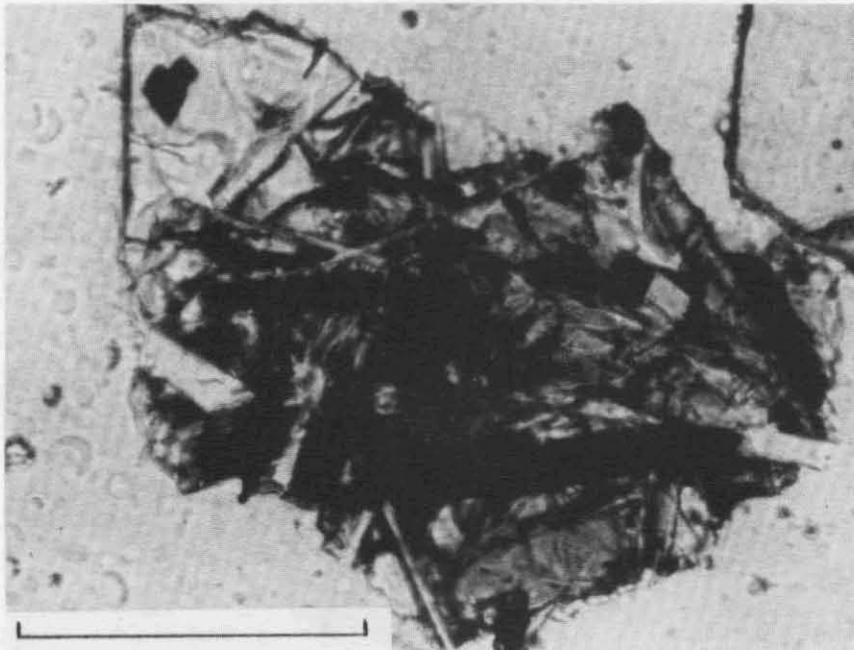
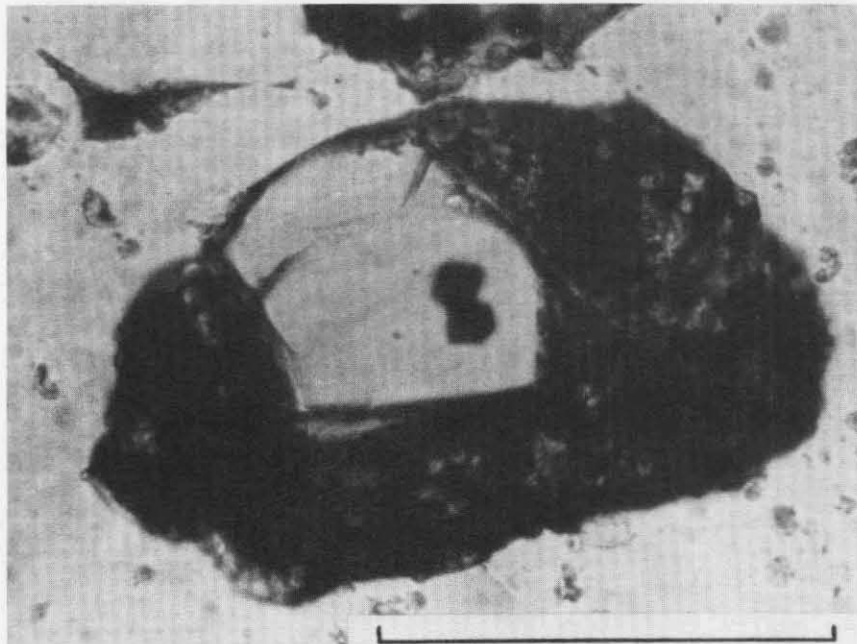
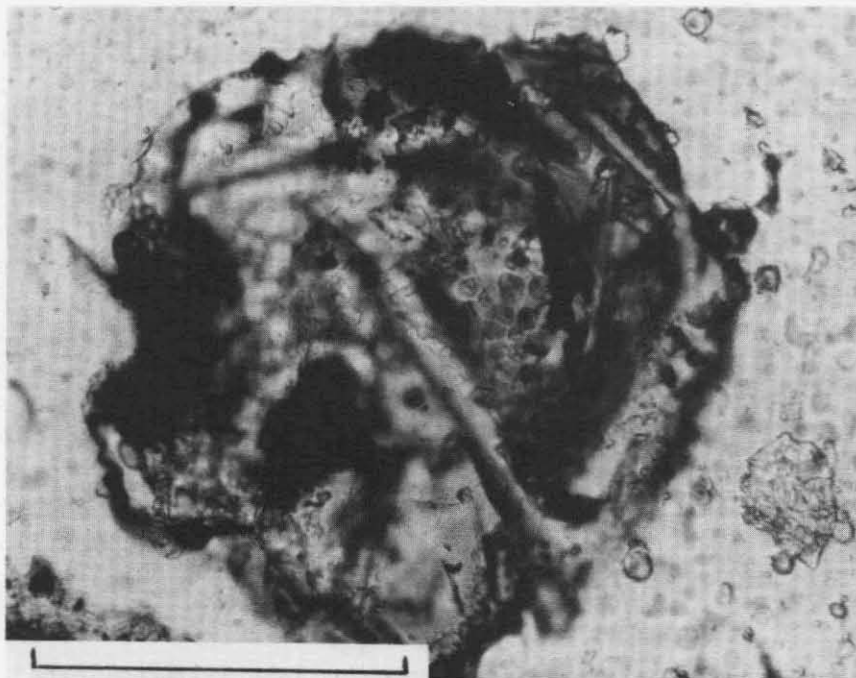


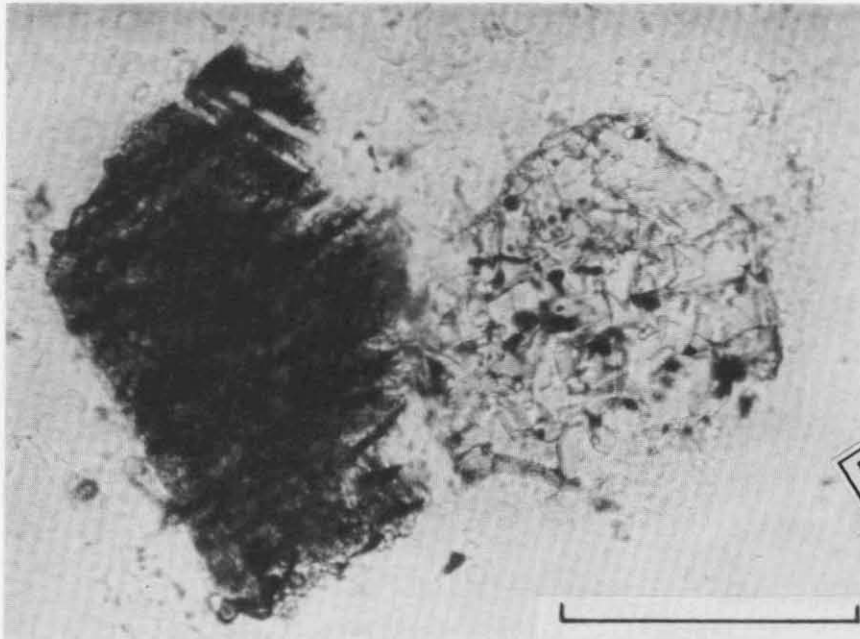
Figure 2. Fine-grained subophitic basalt fragment consisting of clinopyroxene (gray) with laths of ilmenite (black) and plagioclase (white). A large olivine crystal (upper left, clear) contains a smaller euhedral opaque grain, probably Cr-spinel. Fragment 318,268; plane polarized light; scale bar 0.1 mm.



**Figure 3.** Very fine-grained olivine microporphyry, containing an olivine microphenocryst (clear) in a dark microcrystalline matrix composed of pyroxene, opaques, and possibly some plagioclase. The two euhedral opaque grains in the olivine crystal are probably Cr-spinel. Fragment 318,372; plane polarized light; scale bar 0.1 mm.



**Figure 4.** Fine-grained basalt fragment containing small blebs of apparently immiscible glass (gray) associated with plagioclase and a light matrix. Fragment 318,229; plane polarized light; scale bar 0.1 mm.



Reproduced from  
best available copy.

Figure 5. Very fine-grained feldspathic fragment (anorthosite?) (right), associated with fine-grained basaltic rock showing apparently oriented (quench?) opaque phases (left). The anorthositic fragment is microgranular and composed chiefly of plagioclase feldspar, apparently with minor pyroxene and opaque phases. Fragment 318,474 (left); plane polarized light; scale bar 0.1 mm.

A few feldspathic rocks show a uniform granular texture (primary?) (Figures 5, 7, 8) and are characterized by a relatively low content of opaques ( $\leq 5$  percent), by a predominance of plagioclase, and, in one analyzed fragment (301,4) by a lower  $\text{TiO}_2$  content in the pyroxene (0-2 wt. percent) than that determined for a few basaltic pyroxenes (2.5 - 4 wt. percent) (Table 2). Area scans of light microbreccia fragments with a defocussed electron beam (Table 2) indicate a range of compositions corresponding to at least 50-75 percent plagioclase, with pyroxene as most of the remainder. Too few analyses were made to establish whether the pyroxene in the feldspathic rocks is consistently lower in Ca than the clinopyroxene in the basaltic rocks.

## SHOCK-METAMORPHIC EFFECTS

### Introduction

The Luna-16 soil fragments display numerous features characteristic of shock metamorphism produced by meteorite impact and virtually identical to features observed in Apollo 11 and 12 material. Two chief types of shock-metamorphic effects were observed: (1) unusual deformational features in

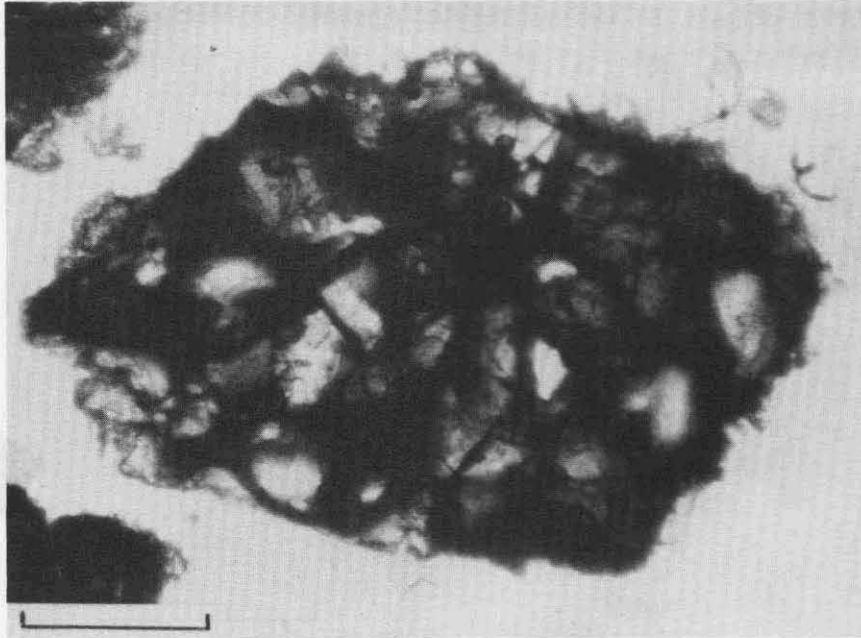


Figure 6A. Shock-metamorphosed(?) microgranular noritic fragment, composed of weakly birefringent pyroxene (gray) and nearly isotropic plagioclase(?) (clear). Dark brown intergranular areas are probably glass produced by incipient post-shock melting along grain boundaries. Fragment 301,4; plane polarized light; scale bar 0.1 mm.

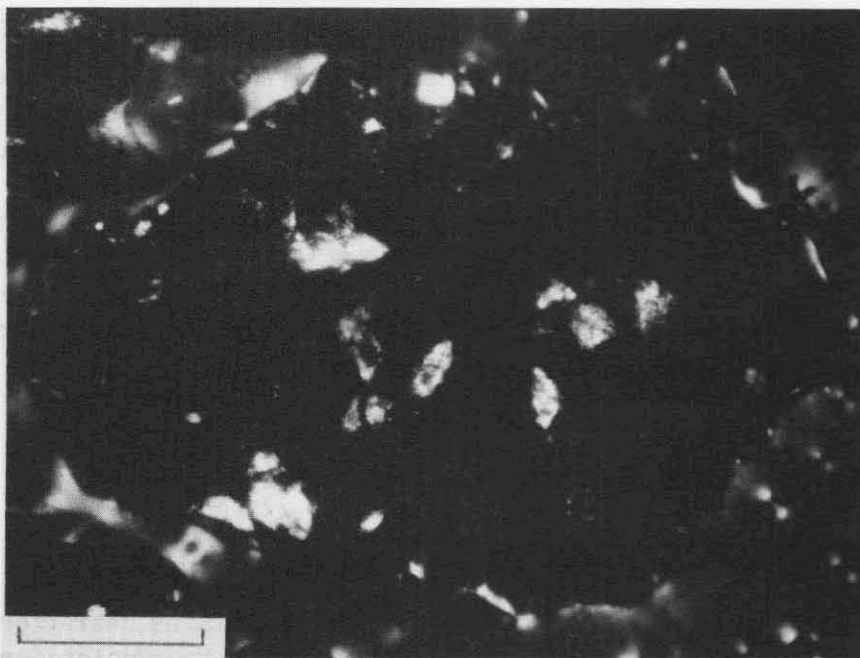


Figure 6B. Same view as Figure 6A; crossed polarizers. Virtually all of the plagioclase and most of the pyroxene grains have little or no birefringence. Most of the grains showing significant birefringence are apparently pyroxene.

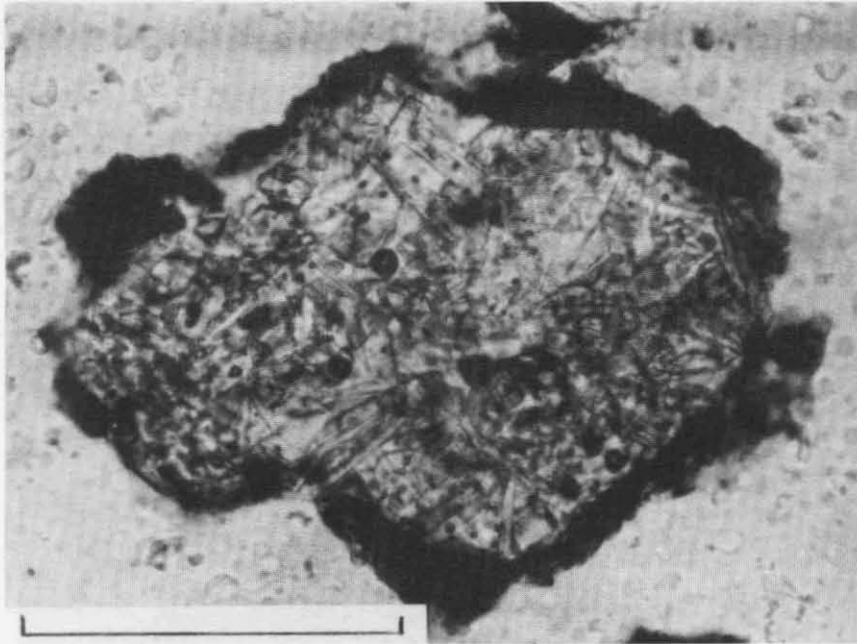


Figure 7. Microgranular feldspathic fragment, surrounded by a thin rim of dark brown, flow-banded glass. The texture of the fragment apparently originated from rapid crystal growth, and the occurrence of spherical bodies (vesicles?) in the fragment suggests an origin by quenching of a feldspar-rich glass, possibly an impact melt. Fragment 318,156; plane polarized light; scale bar 0.1 mm.

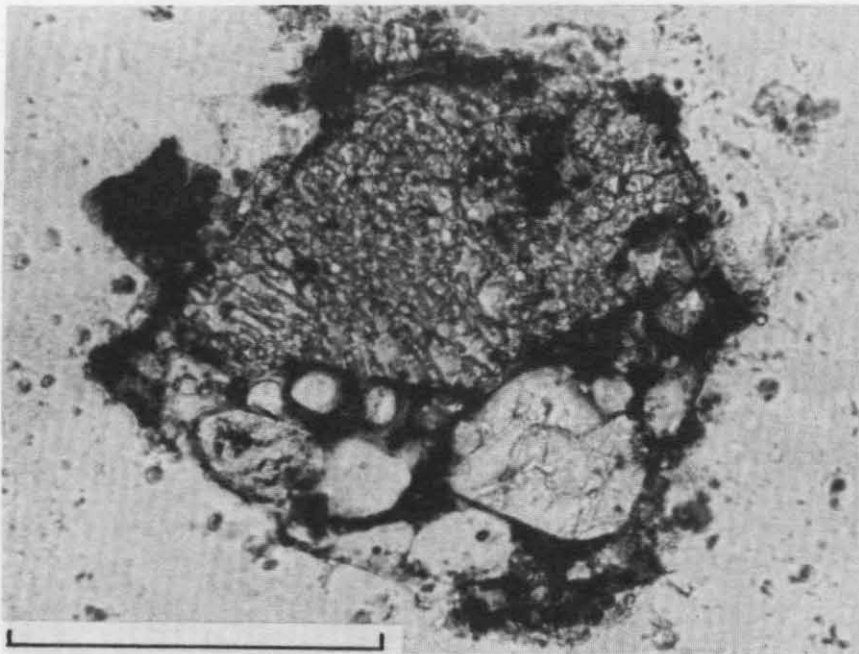


Figure 8. Fragment of plagioclase-pyroxene rock (norite?), contained in a glassy breccia composed of smaller mineral fragments in a matrix of yellow-brown to dark-brown glass. The minerals in the noritic fragment are highly intergrown, forming an almost micrographic texture. Fragment 318,63; plane polarized light; scale bar 0.1 mm.

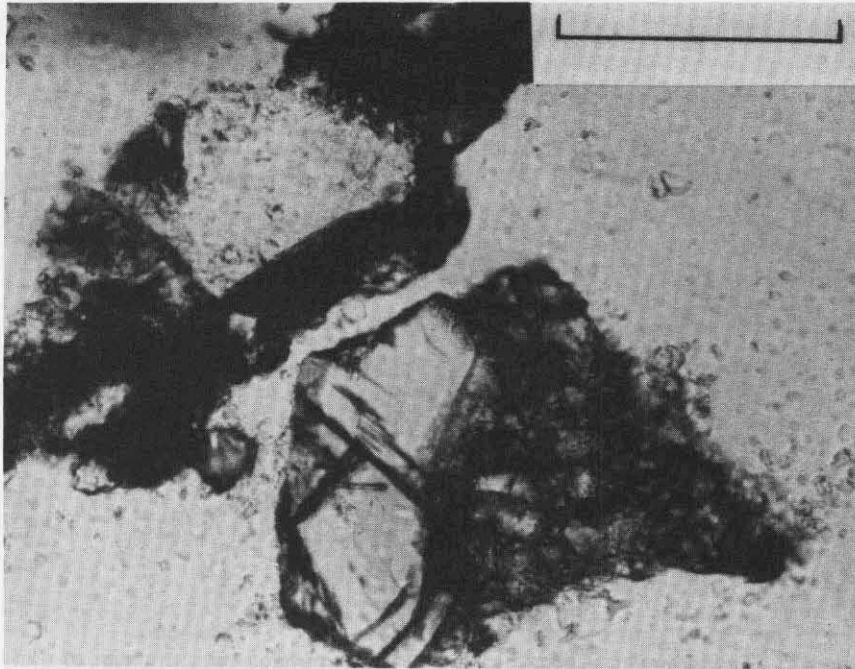


Figure 9A. Two breccia fragments, showing complicated relationships between dark (basaltic) and light (feldspathic) materials. In one fragment (upper left), a clast of anorthosite microbreccia (light) is enclosed in dark basaltic fragmental material. The other fragment contains a large pyroxene crystal in a matrix of light feldspathic microbreccia. Fragments 318,131-2; plane polarized light; scale bar 0.1 mm.

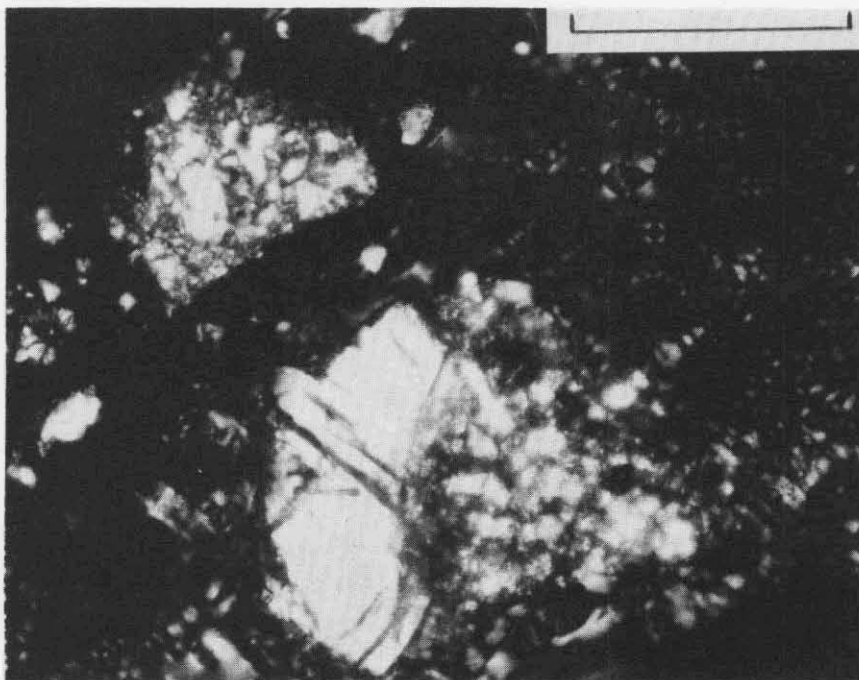


Figure 9B. Same view as Figure 9A; crossed polarizers. Note that both the anorthosite fragment (upper left) and the feldspathic microbreccia (lower right) have similar textures consisting of larger plagioclase grains in a finer microcrystalline matrix.

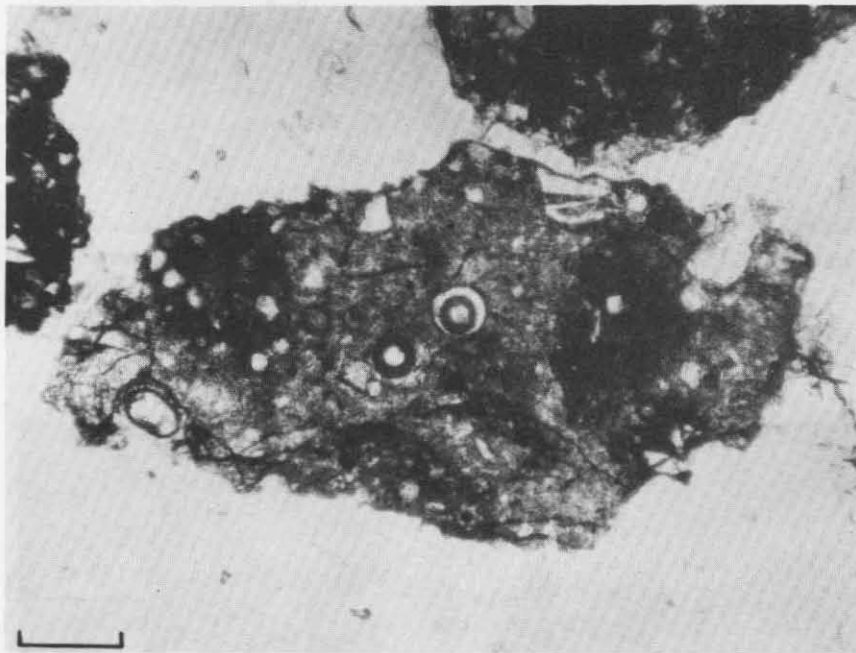


Figure 10. Light feldspathic fragment consisting of small mineral fragments (plagioclase and pyroxene) in a mottled matrix of vesicular, partly devitrified brownish glass. Fragment 301,26; plane polarized light; scale bar 0.1 mm.

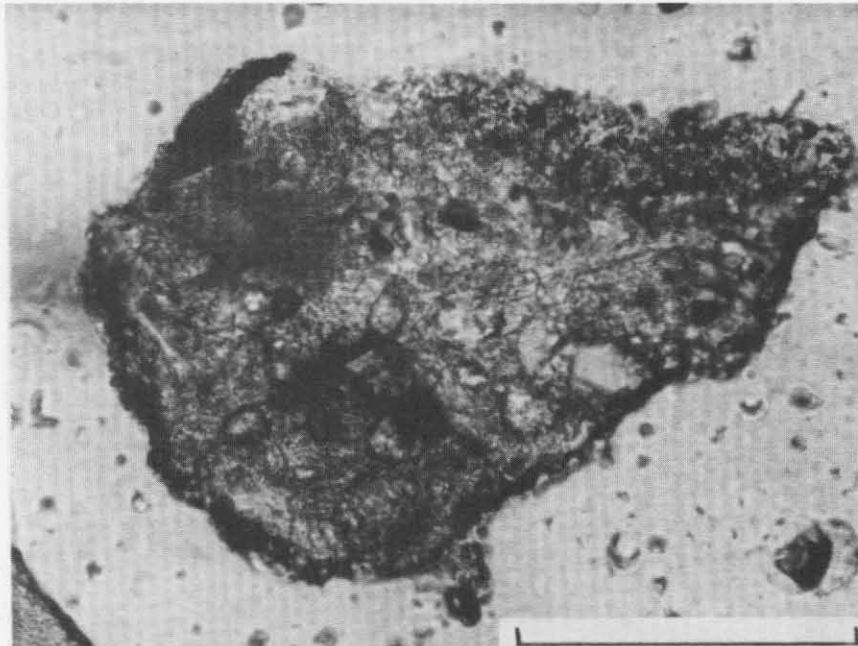


Figure 11A. Light microgranular feldspathic fragment, composed of clear angular plagioclase fragments in a finely-crystalline matrix which also contains isolated darker aphanitic areas. Fragment 318,434; plane polarized light; scale bar 0.1 mm.

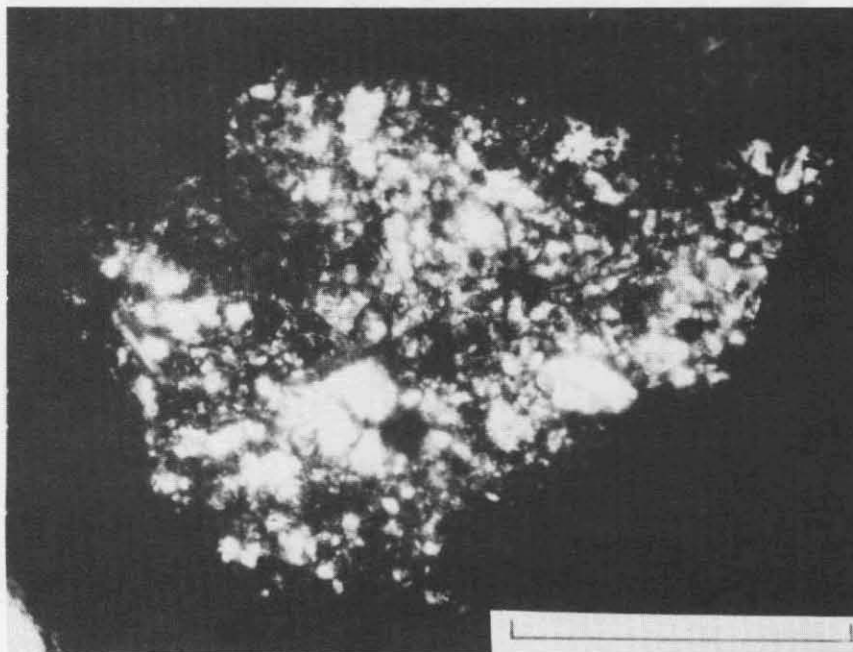


Figure 11B. Same view as Figure 11A; crossed polarizers. The rock consists of variously-sized feldspar crystals in a matrix of fine-grained material. Note that the dark inclusion (upper left) is only slightly crystalline and may possibly be an included glass-rich fragment.

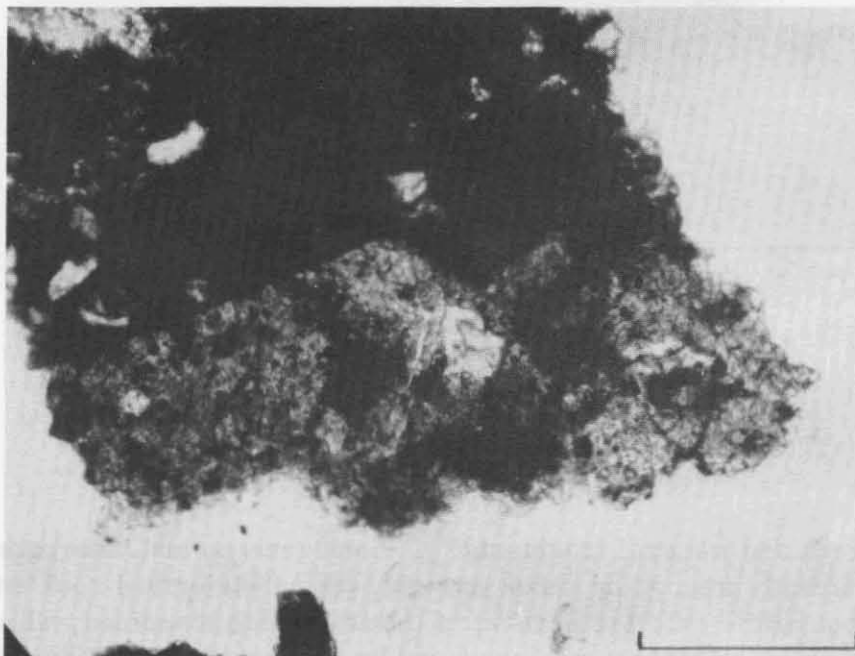


Figure 12. Angular fragments of light microcrystalline feldspathic material enclosed in a matrix of darker microbreccia, probably of basaltic composition. Fragment 301,72; plane polarized light; scale bar 0.1 mm.

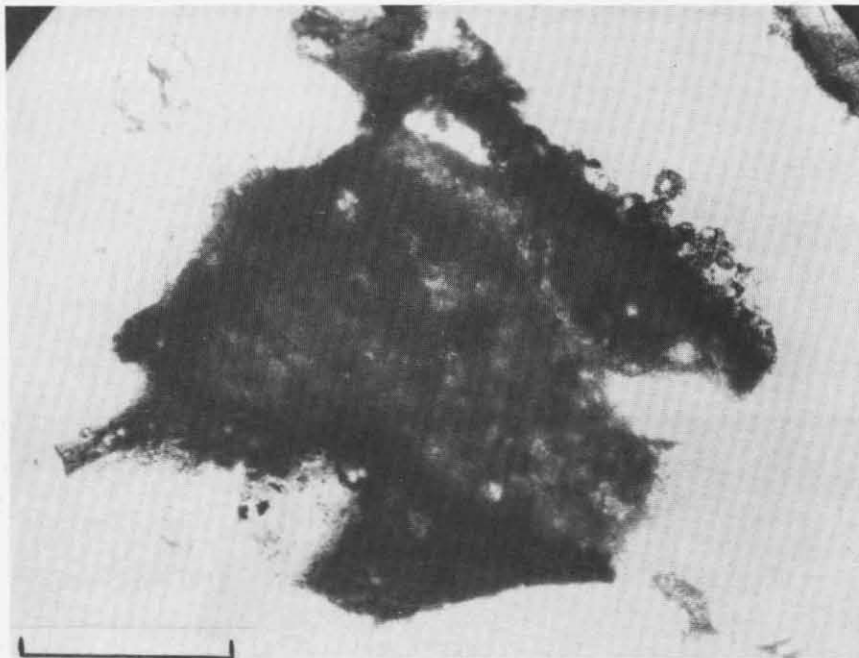


Figure 13. Composite fragment consisting of an angular core of light-brown microcrystalline feldspathic material, surrounded by a thin rim of dark-brown, heterogeneous, flow-banded glass of probable basaltic composition. The texture suggests earlier transport of the feldspathic material to the general area, followed by an impact event which dislodged the feldspathic fragment and coated it with impact-produced basaltic glass produced at the same time. Fragment 301,6; plane polarized light; scale bar 0.1 mm.

individual rock and mineral fragments; (2) homogeneous and heterogeneous glasses apparently formed by shock melting. Shock-deformed rock and mineral fragments constitute only 1-2 percent of the fragments examined, while glasses and glass-bearing microbreccias produced by shock melting and mixing constitute as much as 70-80 percent. Both percentages are comparable to those observed in Apollo 11 samples (2-7, 17, 18).

#### Shocked Rock and Mineral Fragments

Shock-metamorphic effects observed in rock and mineral fragments from the Luna-16 sample include deformation twinning, development of multiple parallel sets of shock lamellae, partial to complete isotropization of minerals, and selective partial melting.

A relative scale of shock deformation based on plagioclase has been established from the Apollo 11 material (2). However, in the small number of shocked fragments observed in the Luna-16 material, pyroxene grains exhibit the greatest variety of shock-produced deformation effects. In order of apparently

Table 2

## Electron Microprobe Analyses of Luna-16 Materials

| Anal. No.         | Fragment | SiO <sub>2</sub> | TiO <sub>2</sub> | Al <sub>2</sub> O <sub>3</sub> | CaO   | MgO   | FeO   | Total  |
|-------------------|----------|------------------|------------------|--------------------------------|-------|-------|-------|--------|
| PYROXENES         |          |                  |                  |                                |       |       |       |        |
| Basalts           |          |                  |                  |                                |       |       |       |        |
| 3                 | 301,1    | 48.24            | 3.51             | 3.83                           | 14.44 | 12.98 | 15.69 | 98.68  |
| 4                 | 301,1    | 47.29            | 3.99             | 4.00                           | 18.09 | 11.84 | 14.23 | 99.49  |
| 7                 | 301,1    | 47.79            | 3.44             | 3.65                           | 18.85 | 11.72 | 13.12 | 98.58  |
| 32                | 301,28   | 49.11            | 2.75             | 3.28                           | 13.63 | 14.81 | 15.48 | 99.06  |
| 33                | 301,28   | 49.90            | 2.81             | 3.38                           | 17.25 | 14.42 | 13.55 | 101.31 |
| Feldspathic rocks |          |                  |                  |                                |       |       |       |        |
| 8                 | 301,4    | 49.02            | 1.43             | 4.32                           | 10.28 | 7.36  | 27.56 | 99.98  |
| 9                 | 301,4    | 48.41            | 0.87             | 16.44                          | 13.98 | 6.07  | 15.11 | 100.87 |
| 11                | 301,4    | 49.20            | 1.19             | 3.73                           | 11.33 | 6.16  | 29.03 | 100.66 |
| 12                | 301,4    | 47.28            | 0.65             | 2.07                           | 15.18 | 6.48  | 20.70 | 92.36  |
| PLAGIOCLASE       |          |                  |                  |                                |       |       |       |        |
| Basalts           |          |                  |                  |                                |       |       |       |        |
| 5                 | 301,1    | 46.35            | 0.22             | 33.15                          | 18.20 | 0.29  | 0.56  | 98.77  |
| 6                 | 301,1    | 46.38            | 0.17             | 33.25                          | 18.36 | 0.25  | 0.58  | 99.00  |
| Feldspathic rocks |          |                  |                  |                                |       |       |       |        |
| 13                | 301,4    | 45.31            | 0.17             | 33.93                          | 18.90 | 0.30  | 1.33  | 99.93  |
| 14                | 301,4    | 47.00            | 0.29             | 29.24                          | 16.96 | 2.70  | 4.16  | 100.34 |
| 49                | 301,73   | 45.95            | 0.09             | 33.95                          | 19.34 | 0.65  | 0.34  | 100.32 |
| 50                | 301,73   | 46.72            | 0.03             | 34.09                          | 19.36 | 0.65  | 0.41  | 101.26 |
| 51                | 301,73   | 45.19            | 0.11             | 34.55                          | 19.27 | 0.44  | 0.29  | 99.85  |

Table 2 (continued)

| Anal. No.                             | Fragment | SiO <sub>2</sub> | TiO <sub>2</sub> | Al <sub>2</sub> O <sub>3</sub> | CaO   | MgO   | FeO   | Total  |
|---------------------------------------|----------|------------------|------------------|--------------------------------|-------|-------|-------|--------|
| Light microbreccias                   |          |                  |                  |                                |       |       |       |        |
| 25                                    | 301,21   | 44.55            | 0.09             | 34.82                          | 19.46 | 0.09  | 0.25  | 99.26  |
| 26                                    | 301,21   | 47.67            | 0.21             | 32.61                          | 18.71 | 0.26  | 1.00  | 100.45 |
| Large single grain fragment           |          |                  |                  |                                |       |       |       |        |
| 38                                    | 301,34   | 46.18            | 0.10             | 34.19                          | 19.10 | 0.47  | 0.31  | 100.35 |
| 39                                    | 301,34   | 45.63            | 0.10             | 34.35                          | 19.08 | 0.35  | 0.32  | 99.83  |
| SILICA                                |          |                  |                  |                                |       |       |       |        |
| 10                                    | 301,4    | 91.50            | 0.33             | 1.37                           | 1.27  | 0.27  | 2.88  | 97.63  |
| OLIVINE                               |          |                  |                  |                                |       |       |       |        |
| 27                                    | 301,21   | 38.44            | 0.20             | 0.24                           | 0.41  | 35.05 | 27.78 | 102.12 |
| GLASSES                               |          |                  |                  |                                |       |       |       |        |
| Clear, colorless glasses              |          |                  |                  |                                |       |       |       |        |
| 28                                    | 301,23   | 43.86            | 0.29             | 27.18                          | 14.94 | 12.20 | 2.96  | 101.42 |
| 29                                    | 301,23   | 44.02            | 0.21             | 27.29                          | 14.57 | 11.93 | 2.83  | 100.85 |
| 30                                    | 301,23   | 43.92            | 0.35             | 27.20                          | 14.92 | 11.52 | 3.00  | 100.92 |
| Clear plagioclase glass (maskelynite) |          |                  |                  |                                |       |       |       |        |
| 42                                    | 301,42   | 44.87            | 0.07             | 34.73                          | 19.11 | 0.23  | 0.15  | 99.15  |
| 43                                    | 301,42   | 45.54            | 0.01             | 34.85                          | 19.31 | 0.18  | 0.18  | 100.08 |
| 44                                    | 301,42   | 45.29            | 0.08             | 34.80                          | 19.53 | 0.11  | 0.20  | 100.00 |
| Annealed plagioclase fragment         |          |                  |                  |                                |       |       |       |        |
| 47                                    | 301,71   | 45.03            | 0.12             | 34.44                          | 19.17 | 0.18  | 0.24  | 99.17  |

Table 2 (continued)

| Anal. No.                                     | Fragment | SiO <sub>2</sub> | TiO <sub>2</sub> | Al <sub>2</sub> O <sub>3</sub> | CaO   | MgO   | FeO   | Total  |
|---|----------|------------------|------------------|--------------------------------|-------|-------|-------|--------|
| Clear devitrified spherule                    |          |                  |                  |                                |       |       |       |        |
| 23  | 301,21   | 43.26            | 0.20             | 28.53                          | 18.91 | 3.02  | 3.32  | 97.25  |
| Dark, heterogeneous, flow-banded glasses      |          |                  |                  |                                |       |       |       |        |
| 16  | 301,15   | 43.50            | 3.54             | 15.23                          | 11.91 | 9.13  | 16.87 | 100.19 |
| 17  | 301,15   | 44.11            | 3.76             | 15.16                          | 11.80 | 8.91  | 15.27 | 99.02  |
| 18  | 301,15   | 43.96            | 3.62             | 15.94                          | 11.96 | 8.52  | 14.63 | 98.62  |
| 34  | 301,33   | 43.78            | 4.25             | 15.14                          | 11.98 | 8.86  | 15.32 | 99.34  |
| 36  | 301,33   | 43.87            | 3.52             | 16.06                          | 12.40 | 8.84  | 15.06 | 99.76  |
| 37  | 301,33   | 44.85            | 3.40             | 16.09                          | 12.41 | 8.89  | 15.02 | 100.66 |
| 41  | 301,40   | 42.71            | 3.17             | 13.82                          | 11.48 | 10.20 | 20.83 | 102.20 |
| 45  | 301,51   | 41.65            | 3.22             | 16.65                          | 12.34 | 9.16  | 16.00 | 99.02  |
| 46  | 301,51   | 43.36            | 3.02             | 16.57                          | 12.52 | 9.19  | 15.14 | 99.81  |
| Dark brown glass in plagioclase-rich fragment |          |                  |                  |                                |       |       |       |        |
| 52  | 301,73   | 46.36            | 0.46             | 7.89                           | 8.62  | 19.19 | 18.76 | 101.29 |
| 53  | 301,73   | 41.60            | 0.51             | 6.62                           | 4.91  | 26.58 | 21.47 | 101.70 |
| 54  | 301,73   | 41.89            | 0.28             | 3.06                           | 2.98  | 34.31 | 21.64 | 104.15 |
| 55  | 301,73   | 47.03            | 0.69             | 9.58                           | 13.91 | 8.81  | 19.88 | 99.91  |
| LIGHT MICROBRECCIAS (area scan analyses)      |          |                  |                  |                                |       |       |       |        |
| 15  | 301,6    | 39.87            | 1.73             | 16.57                          | 11.11 | 7.68  | 12.56 | 89.51  |
| 24  | 301,21   | 45.96            | 0.57             | 23.65                          | 14.00 | 7.53  | 7.89  | 99.59  |
| 31  | 301,26   | 47.00            | 1.34             | 22.03                          | 14.49 | 5.50  | 9.11  | 99.48  |
| 40  | 301,37   | 43.84            | 1.18             | 18.20                          | 13.08 | 6.54  | 8.75  | 91.60  |
| 48  | 301,72   | 41.31            | 1.38             | 17.65                          | 11.04 | 7.73  | 11.54 | 90.66  |

increasing shock pressures, these include: (1) deformation twin lamellae, probably parallel to (001) (25) (Figures 14-16); (2) multiple sets of finer parallel lamellae, apparently produced at higher shock pressures (3, 26) (Figure 17); (3) extreme mosaicism (Figures 16, 18); (4) possible partial isotropization (Figures 19, 20); (5) possible selective melting (Figure 21).

Only a few shock-deformed fragments of plagioclase were observed. Multiple planar features (shock lamellae) were observed in one fragment (311, 25). Completely isotropic plagioclase (maskelynite) was identified in another (Figure 22). The occurrence of colorless glasses with a plagioclase-rich composition (e.g., see Figure 33) implies the existence of shock-melted plagioclase in the Luna-16 material as well (e.g., 2).

Neither shock-produced deformation twins in ilmenite (27) or deformation structures in olivine (25) were observed in the Luna-16 material examined. The presence of shock effects in both pyroxene and plagioclase implies that analogous shock effects are present in other minerals and should be observed with more extensive study.

Only three shocked basaltic rock fragments were observed (Figures 23, 24). In two specimens (Figures 23, 24) fractured pyroxene is associated with isotropic,

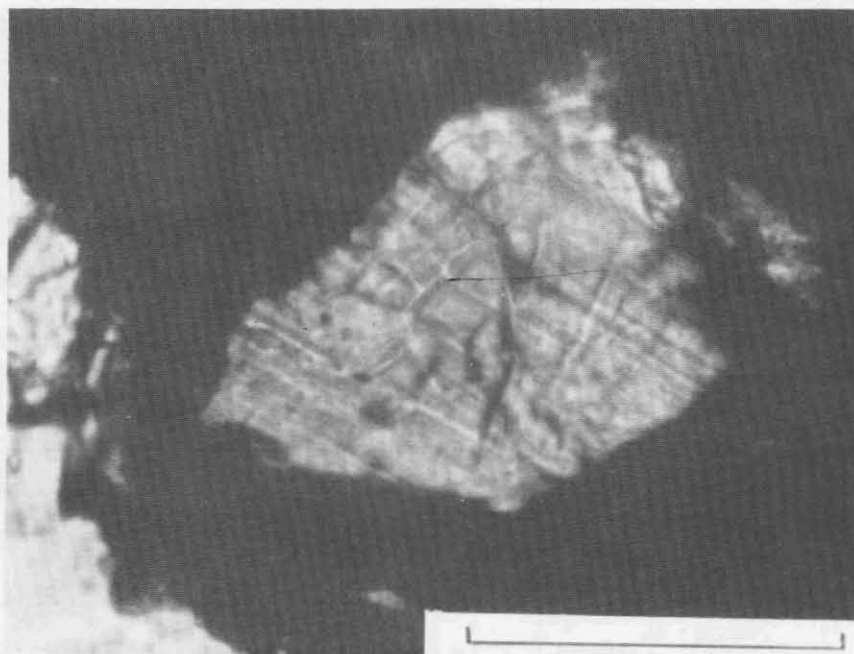


Figure 14. Apparent deformation twin lamellae in a weakly shocked pyroxene crystal in dark microbreccia (alternating light and dark lines running WNW to ESE across the crystal). Fragment 301,68; plane polarized light; scale bar 0.1 mm.

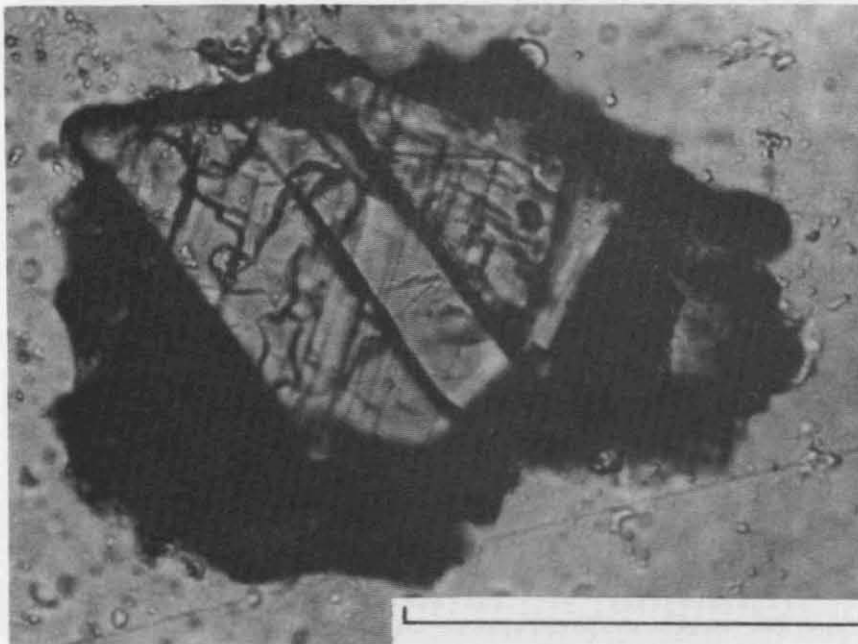


Figure 15A. Weakly shocked pyroxene crystal in dark microbreccia. The crystal displays both cleavage (dark lines, NW-SE) and deformation twin lamellae (lighter parallel lines, NE-SW). Fragment 318,6; plane polarized light; scale bar 0.1 mm.

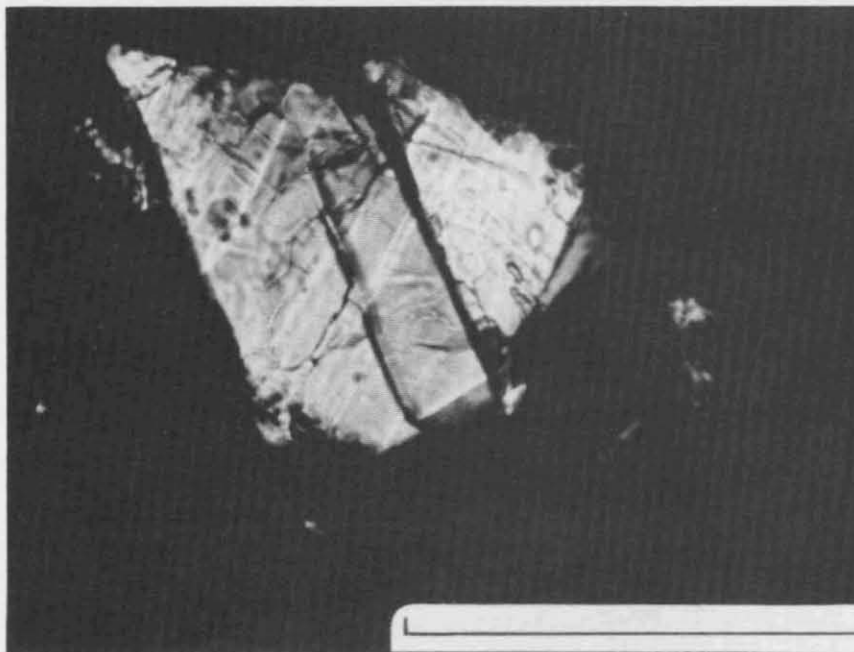


Figure 15B. Same view as Figure 15A; crossed polarizers. Deformation twin lamellae appear as bright lines. Extinction is mildly undulose but not mosaic.

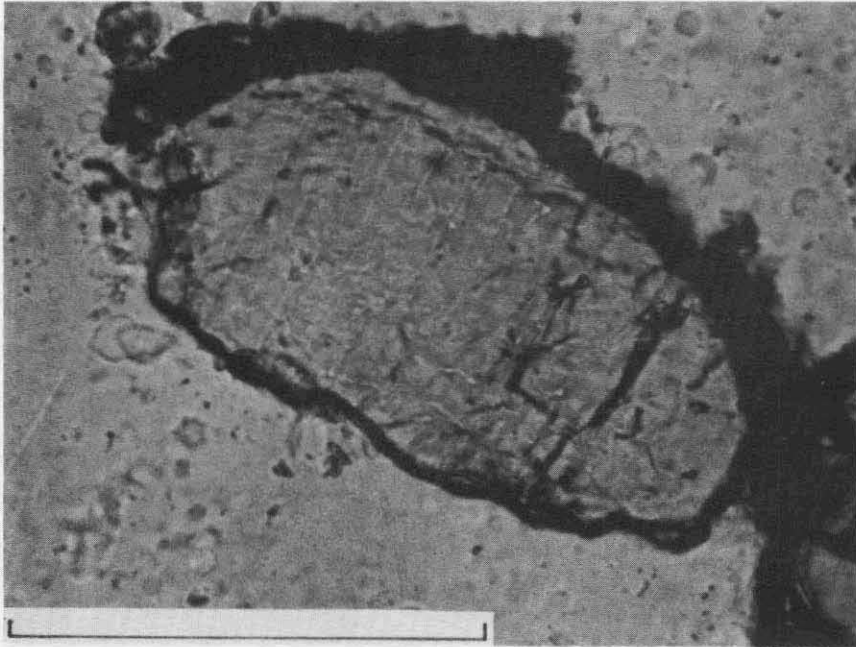


Figure 16A. Weakly shocked pyroxene crystal attached to dark microbreccia material. Features that are apparently deformation twin lamellae appear as very thin light lines running NE-SW. A second set of features (shock lamellae?) is poorly developed in an E-W direction at a high angle to the twin lamellae. Fragment 318,46; plane polarized light; scale bar 0.1 mm.

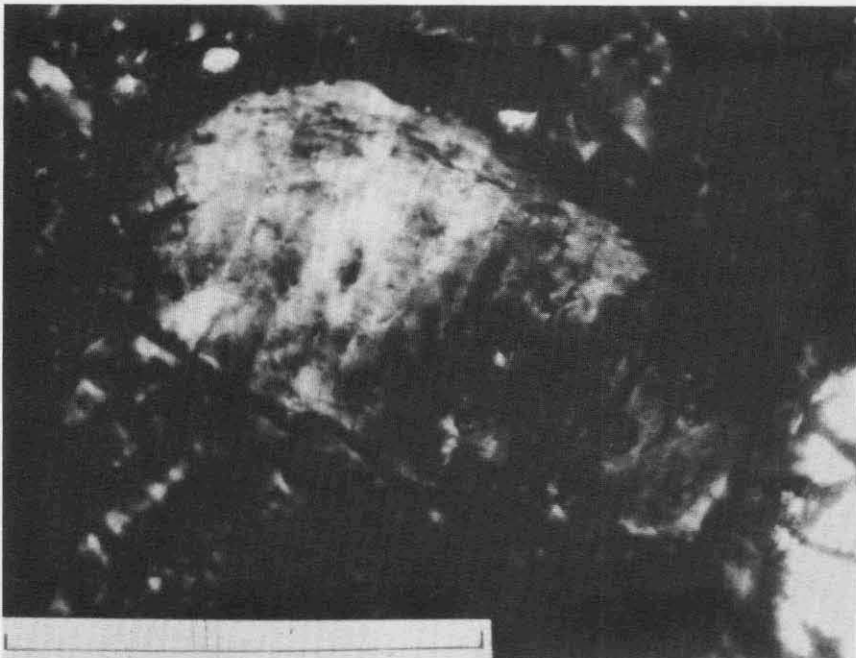


Figure 16B. Same view as Figure 16A; crossed polarizers. Extinction in the crystal is highly mosaic, more strongly so than in the crystal shown in Figure 15.



Figure 17A. Well-developed multiple sets of parallel shock lamellae in a pyroxene crystal. At least six separate sets can be distinguished. Fragment 318,512; plane polarized light; scale bar 0.1 mm.

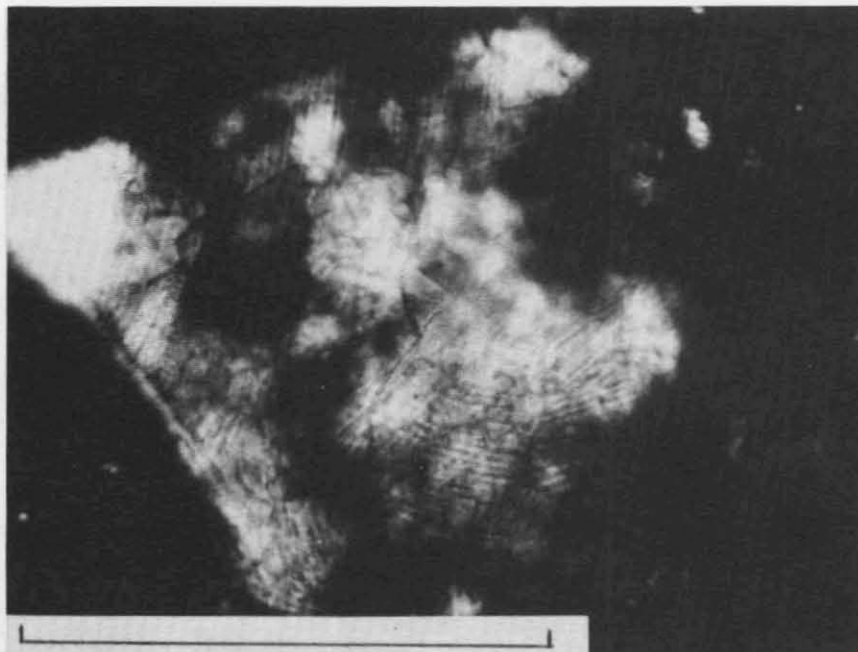


Figure 17B. Same view as Figure 17A; crossed polarizers. Extinction is slightly mosaic in the crystal, but the dark areas are not isotropic.

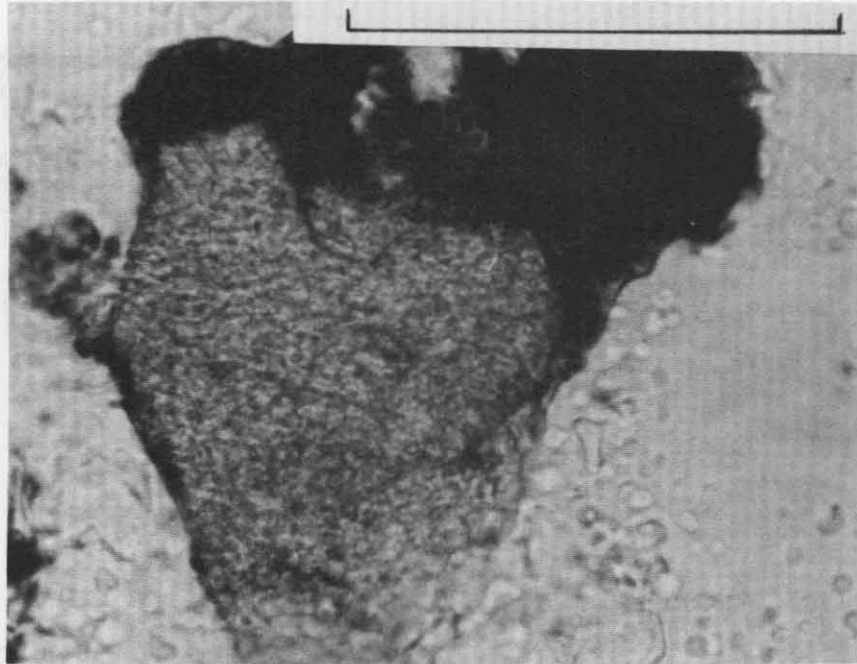


Figure 18A. Strong mosaic extinction in a pyroxene grain in dark microbreccia. Planar shock lamellae are poorly developed in the upper left part of the crystal (running NW-SE), but cannot be recognized elsewhere. Fragment 318,182; plane polarized light; scale bar 0.1 mm.

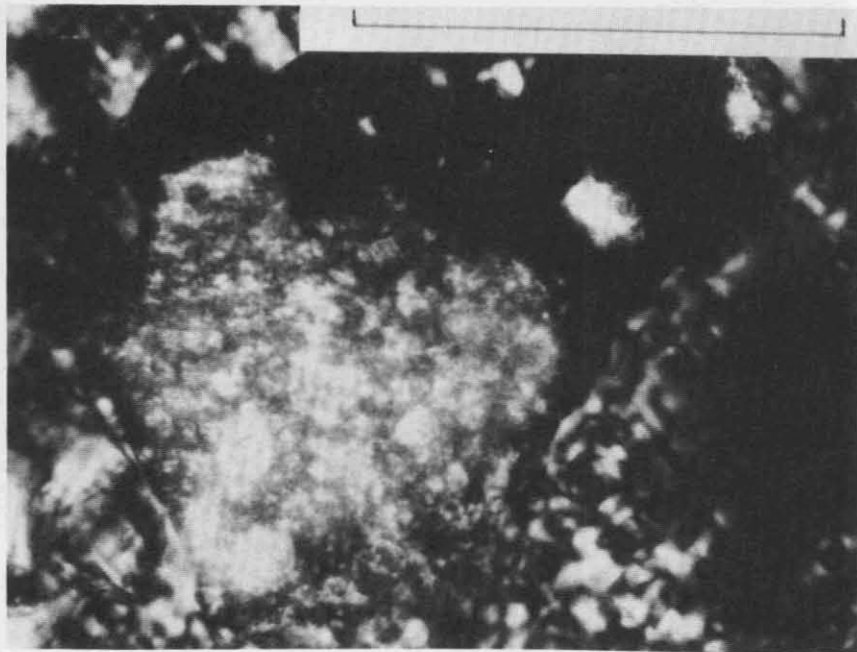


Figure 18B. Same view as Figure 18A; crossed polarizers. Extinction in the crystal is very irregular and patchy and highly mosaic, but definite isotropic areas are not present.

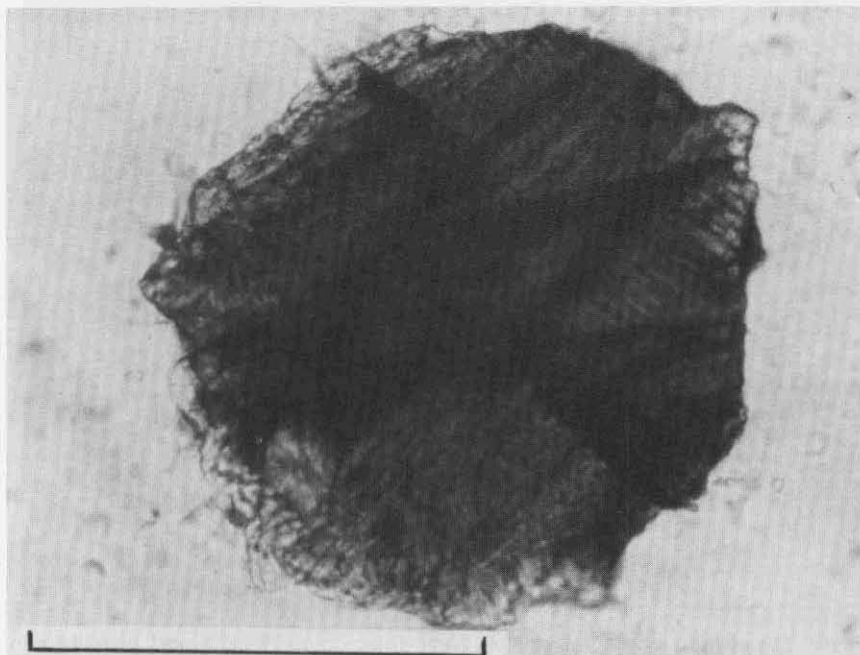


Figure 19. Highly shocked, partially isotropized(?) pyroxene crystal. Several sets of planar shock lamellae are well developed in various parts of the crystal. Dark material occurring along apparent veinlike fractures may represent areas of incipient isotropization or melting of the crystal. Fragment 318,544; plane polarized light; scale bar 0.1 mm.

plagioclase (maskelynite), similar to associations in Apollo 11 rocks (2, 4, 6). In the third basalt fragment, plagioclase is only partially isotropic, but part of the fragment has fused to an orange-brown glass apparently generated by the post-shock melting of opaque phases (Figure 25). In this specimen, the formation of glass, combined with the rapid quench implied by the preservation of plagioclase, is good evidence for shock-induced melting.

#### Impact-Produced Glasses

A variety of glasses occurs in the Luna-16 sample, both as individual fragments and in the matrix of microbreccia fragments. The glasses are virtually identical to those described from Apollo 11 and 12 material and are almost certainly of impact origin. The glasses display several features characteristic of origin by shock-induced melting:

- (1) Diversity in color (and presumably in chemical composition) (7). The colors of dense, homogeneous glass fragments range from colorless through light green, greenish brown, and brown, to dark reddish brown and brownish black. Several free-form fragments (spherules, droplets, etc.) were observed (Figures 26-28).

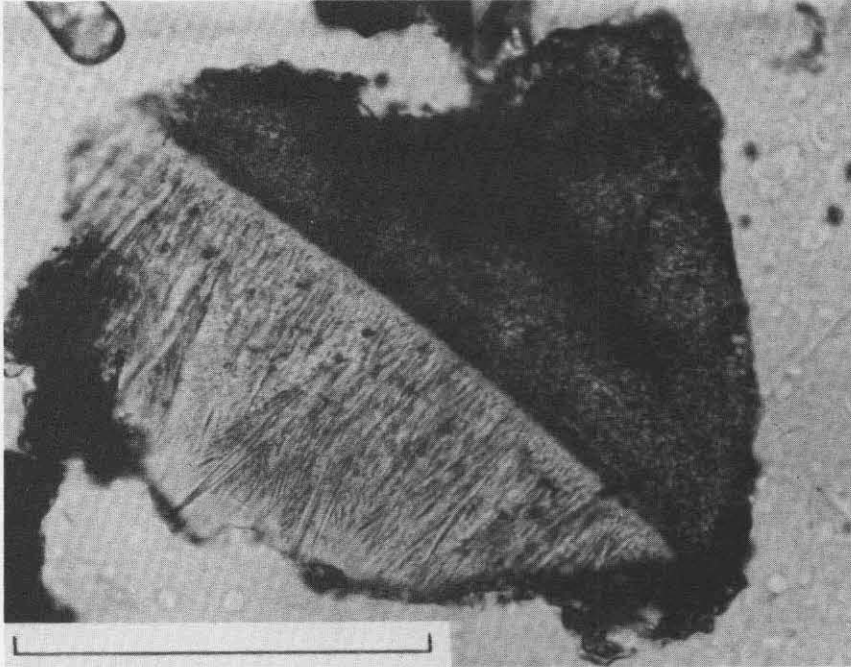


Figure 20A. Sharp contact between clear (plagioclase?) glass and a red-brown pyroxene(?) crystal which shows intense mosaic extinction and partial isotropization along dark veinlike regions. The plagioclase area, which was either maskelynite or shock-melted glass, is now partly devitrified to radiating and sheaflike plagioclase microlites. Fragment 318,362; plane polarized light; scale bar 0.1 mm.

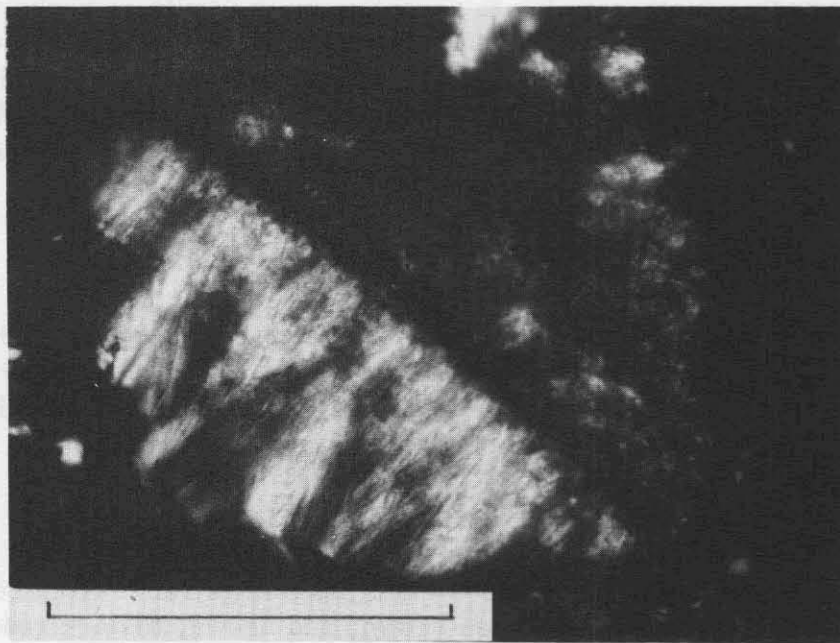


Figure 20B. Same view as in Figure 20A; crossed polarizers. Note devitrification of plagioclase glass area, while adjacent pyroxene(?) region is isotropic in the dark veinlike areas and finely microcrystalline (mosaic extinction?) elsewhere.

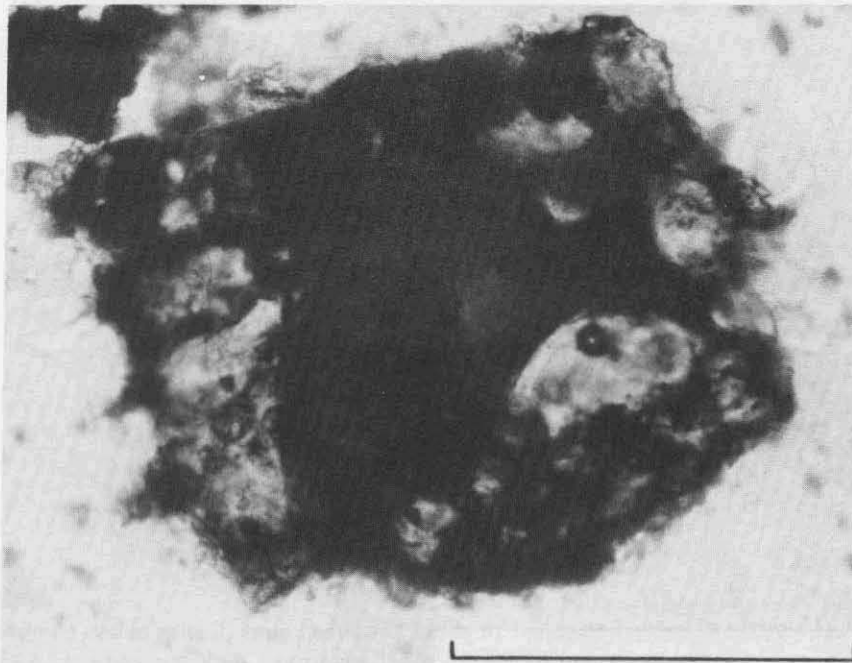


Figure 21. Heterogeneous glassy fragment, composed of a red-brown core which may be incipiently shock-melted pyroxene, surrounded by irregular clear areas which are apparently partly melted plagioclase. The red-brown material in the center is isotropic. If the identification is correct, this fragment represents the highest stage of recognizable shock metamorphism observed in pyroxene. Fragment 318,283; plane polarized light; scale bar 0.1 mm.

- (2) Brightly reflecting spherules (Ni-Fe or troilite?) commonly present in the flowed heterogeneous glasses (Figure 27B) and in microbreccia matrices.
- (3) Distinctive flow lines (schlieren) in heterogeneous glasses, composed of bands of glasses of different colors and implying partial mixing of materials of different compositions (Figures 29-31).
- (4) Intimate mixing of glass and diverse rock fragments, some of which show shock-metamorphic effects (Figures 30-34).
- (5) Incipient fusion of some mineral grains included in glassy fragments (Figures 33, 34), indicating superheating of the glass and disequilibrium between crystals and glass.

The character of the glassy material in the Luna-16 sample is virtually identical to that observed in the Apollo specimens (e.g., 7) and almost certainly reflects origin by meteorite impact. The preponderance of impact-produced

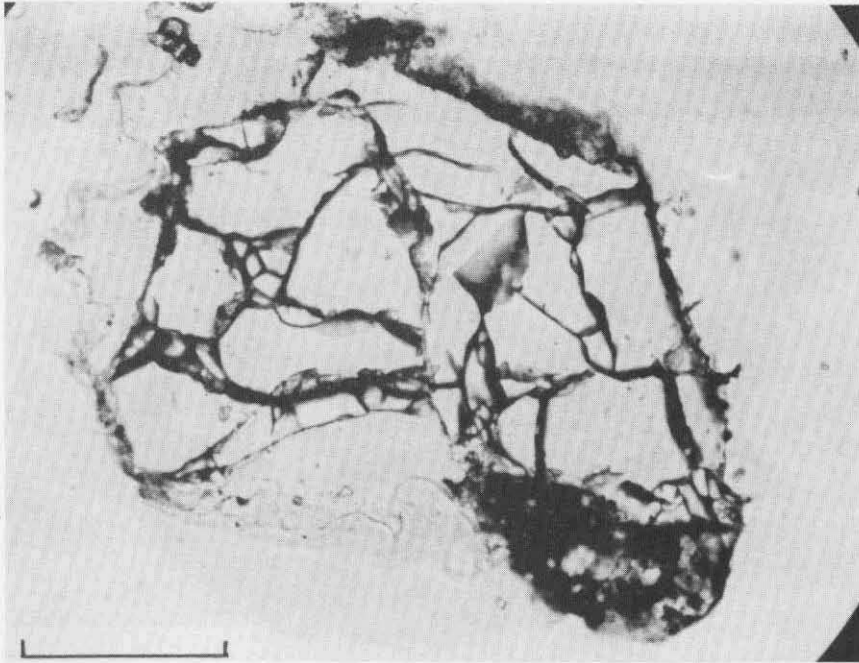


Figure 22A. Fractured fragment of shock-produced glass of plagioclase composition (maskelynite) with a small amount of dark microbreccia adhering at lower right. Fragment 301,42; plane polarized light; scale bar 0.1 mm.

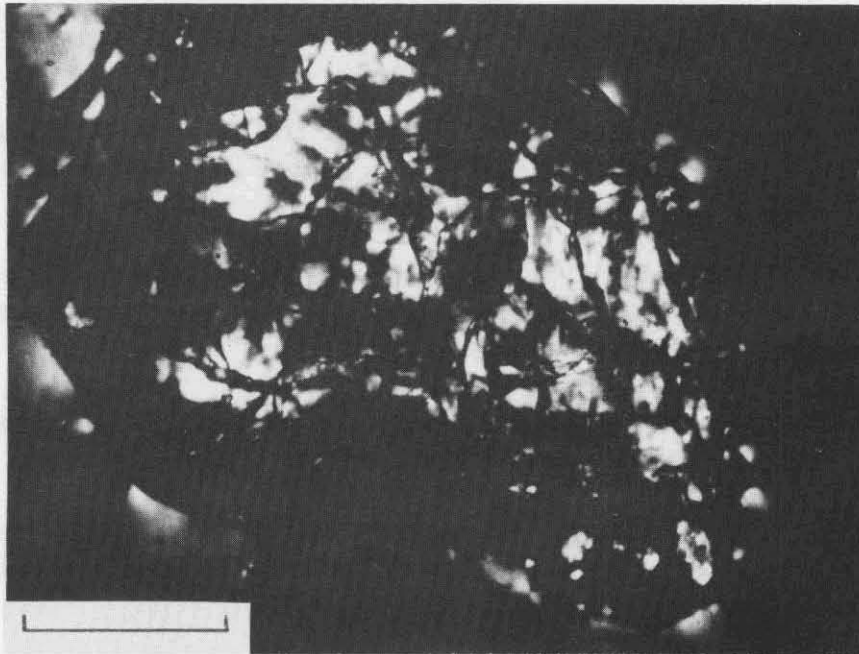
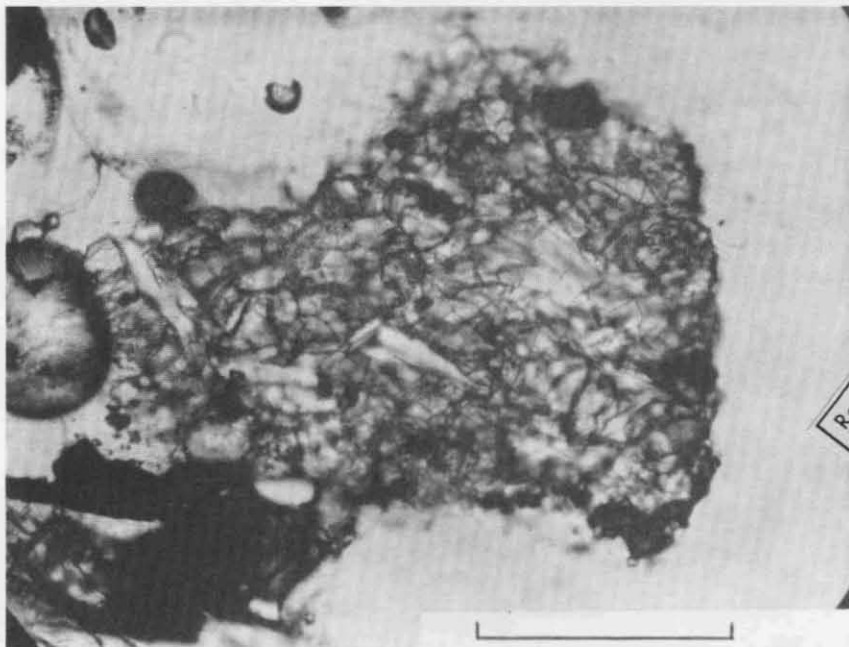


Figure 22B. Same view as Figure 22A; crossed polarizers. The fragment is largely isotropic with some internal birefringence. The birefringence pattern is patchy and irregular rather than spherulitic, suggesting that the birefringence may arise from relict crystalline structure in the maskelynite rather than from post-shock devitrification.



Reproduced from  
best available copy.

Figure 23A. Shock-metamorphosed basalt fragment, composed of fractured clinopyroxene with isotropic plagioclase laths (maskelynite). Fragment 315,53; plane polarized light; scale bar 0.1 mm.

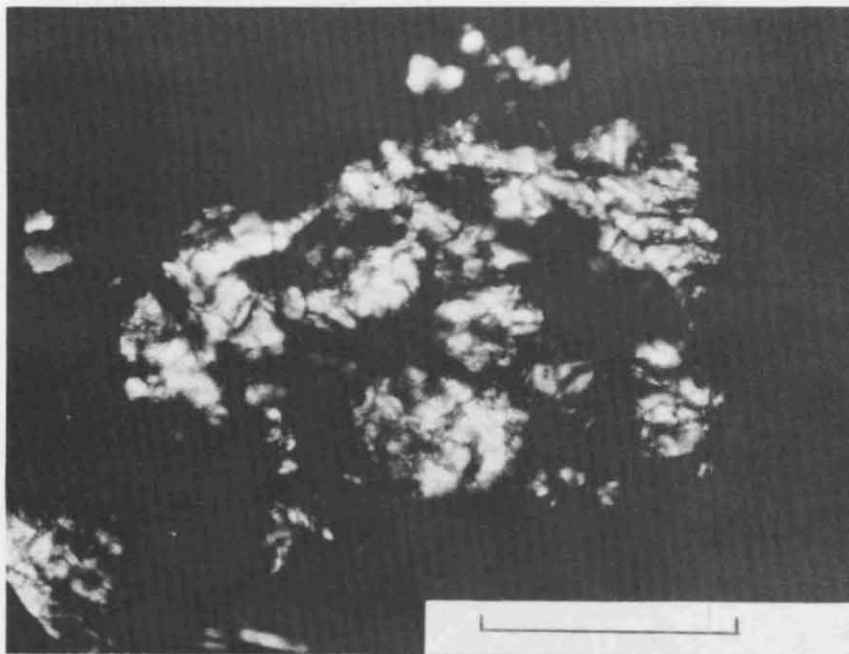


Figure 23B. Same view as Figure 23A; crossed polarizers. The pyroxene remains birefringent and lacks extremely mosaic extinction; plagioclase areas are dark and isotropic.

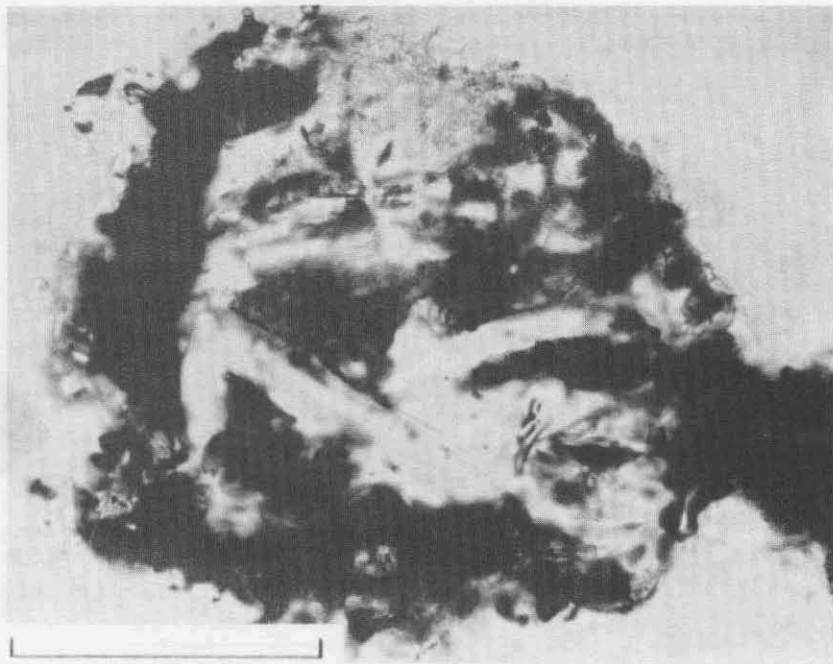


Figure 24A. Plagioclase-bearing shock-metamorphosed basalt fragment with adhering selvages of dark microbreccia material. The fragment is composed of isotropic plagioclase laths (maskelynite) with intergranular crystals of pyroxene that display fracturing and birefringence. Fragment 315,130; plane polarized light; scale bar 0.1 mm.



Figure 24B. Same view as Figure 24A; crossed polarizers. Pyroxene crystals show birefringence, while larger plagioclase laths are dark and isotropic.

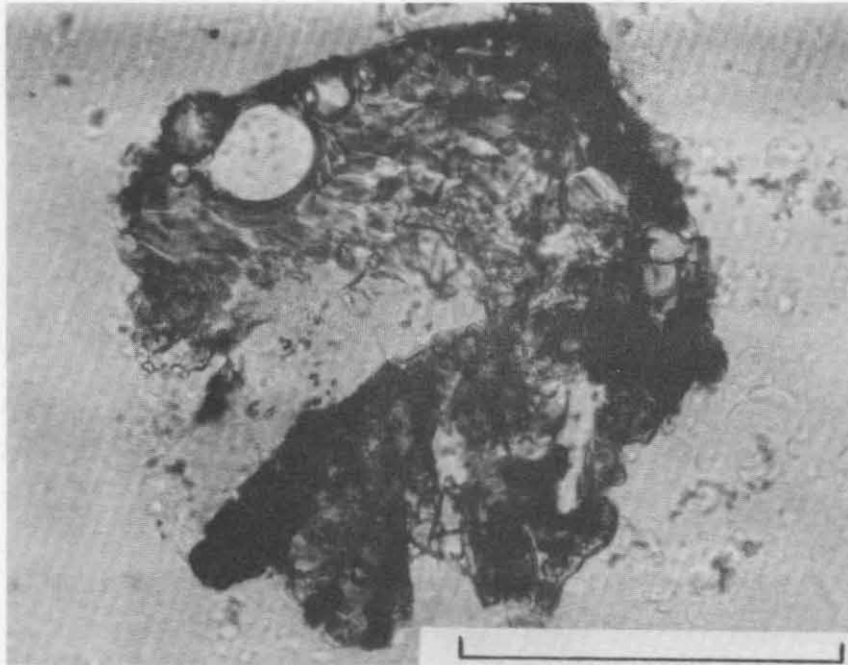


Figure 25A. Partly shock-melted basalt fragment. The unaltered basalt (lower part of fragment), is composed of plagioclase (white), pyroxene (gray), and opaques (black). The crystalline texture of the basalt grades into heterogeneous, vesicular, flow-structured, orange-brown glass (upper part), probably produced by partial melting of opaque phases and plagioclase. The plagioclase grain (white, lower left) is apparently being absorbed into the glass. Fragment 318,460; plane polarized light; scale bar 0.1 mm.

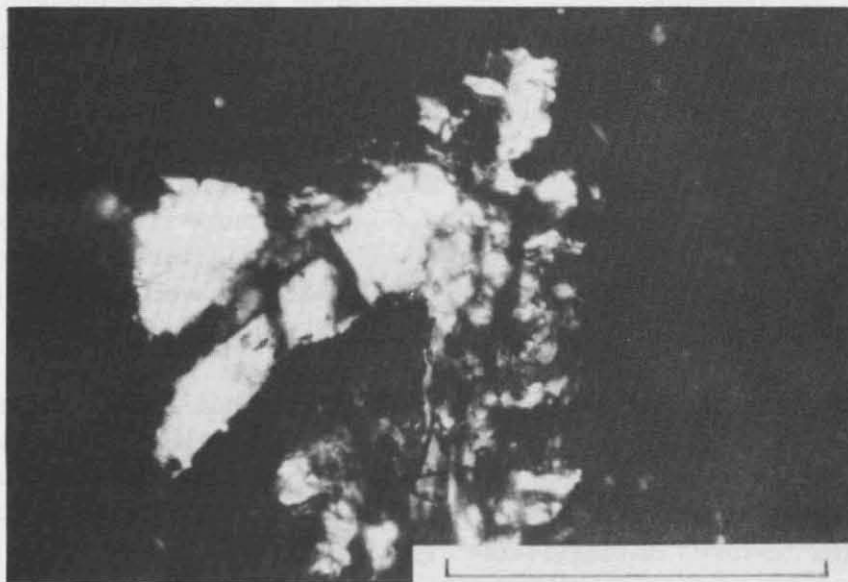


Figure 25B. Same view as Figure 25A; crossed polarizers. The birefringent plagioclase shows two dark isotropic bands across the crystal, possibly produced by shock or by incipient post-shock fusion associated with formation of the glass.

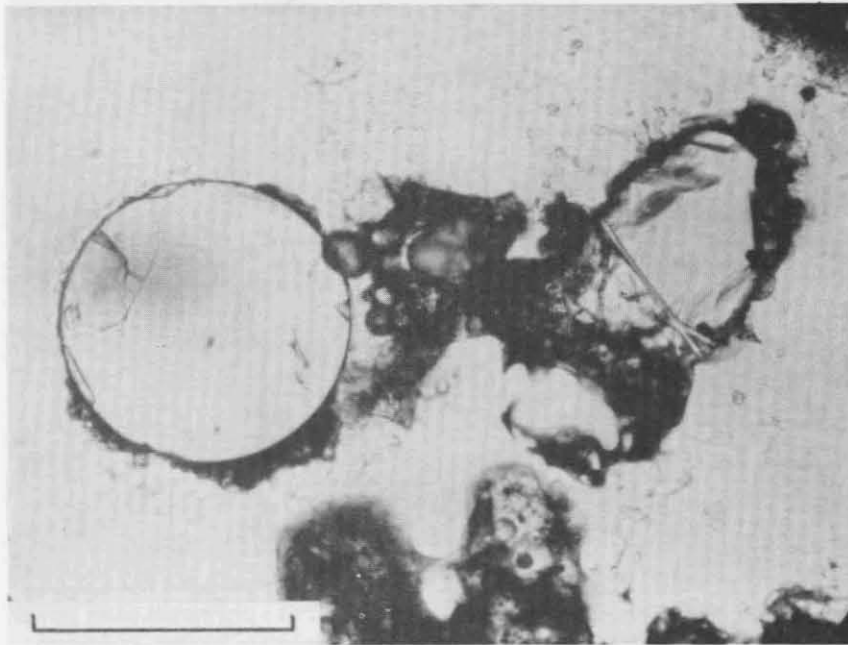


Figure 26. Colorless glass spherule (left) and large pyroxene crystal (right) cemented by dark vesicular filaments of glass containing smaller mineral fragments. Fragment 318,451; plane polarized light; scale bar 0.1 mm.

glasses over shocked rock and mineral fragments is likewise consistent with observations on the returned Apollo samples.

Some glass fragments in the Luna-16 sample also exhibit quenching and devitrification textures similar to those reported in Apollo material (e.g., 2, 3, 4). The textures suggest that crystal growth took place both during rapid cooling in the liquid state (quenching) and in the solid state (devitrification).

The light green to greenish brown fragments contain equant to slightly tabular crystals that may be olivine (Figure 35). The more strongly colored yellow-brown to dark brown fragments display elongate, highly birefringent crystals and microlites, probably pyroxene (Figures 36-38), as well as parallel and dendritic growths of quench opaques (e.g., 3, 27) (Figure 39).

The colorless to pale green glasses with plagioclase-rich compositions (7) are generally less crystallized. Where present, crystallization has apparently taken place in the solid state and is strongly controlled by the shape of the fragment. The most common devitrification effect is the development of radiating or spherulitic textures of plagioclase crystals (Figures 20, 40).

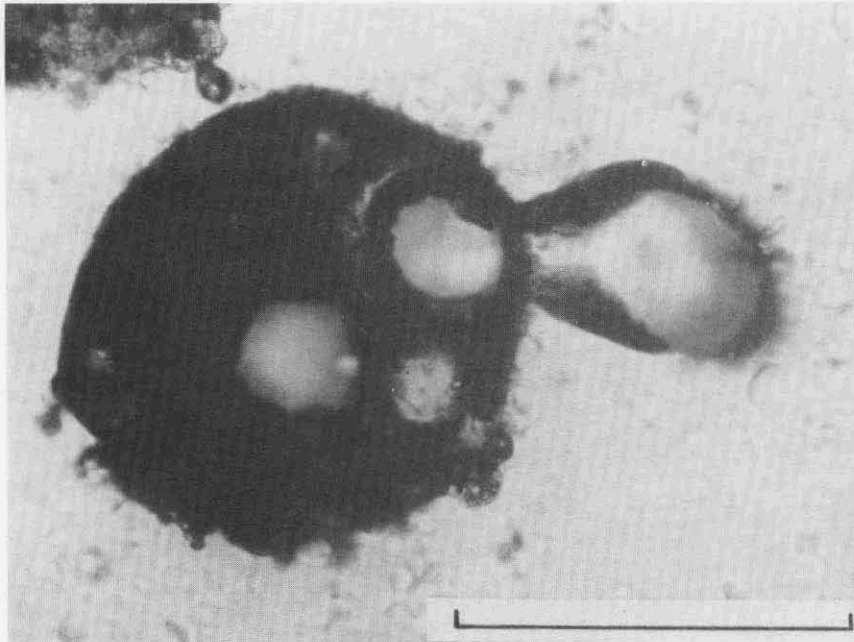


Figure 27A. Vesicular spherule of dark-brown, nearly opaque glass containing mineral fragments. Note the secondary bubble-like structure at upper right, probably formed by venting of gas from the adjacent vesicle in the spherule before complete solidification. Fragment 318,553; plane polarized light; scale bar 0.1 mm.

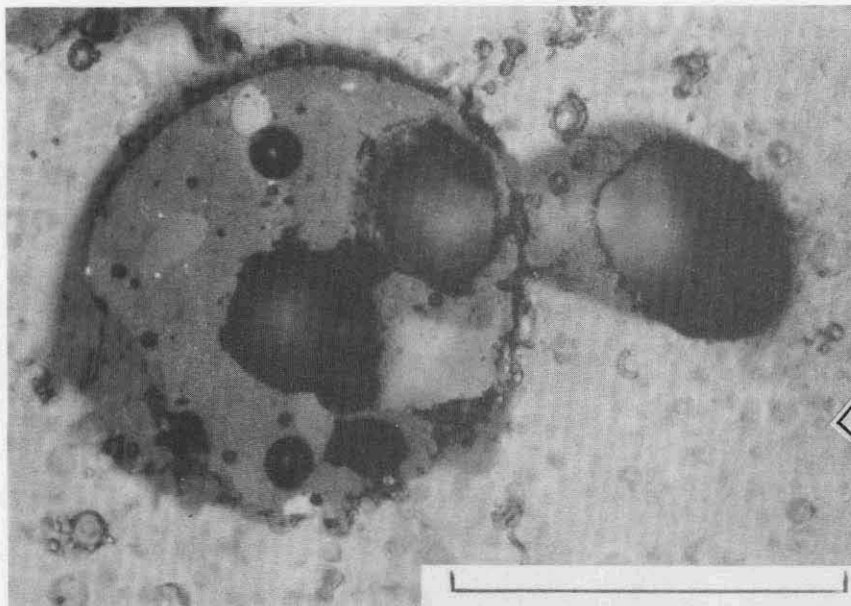


Figure 27B. Same view as Figure 27A; reflected light. The dark glass spherule contains elliptical, partly-digested mineral inclusions, apparently pyroxene (dark gray, left) and an opaque phase (lighter gray, top). Small Ni-Fe spherules in the glass appear as very small bright specks, especially at the left side of the spherule.

Reproduced from  
best available copy.

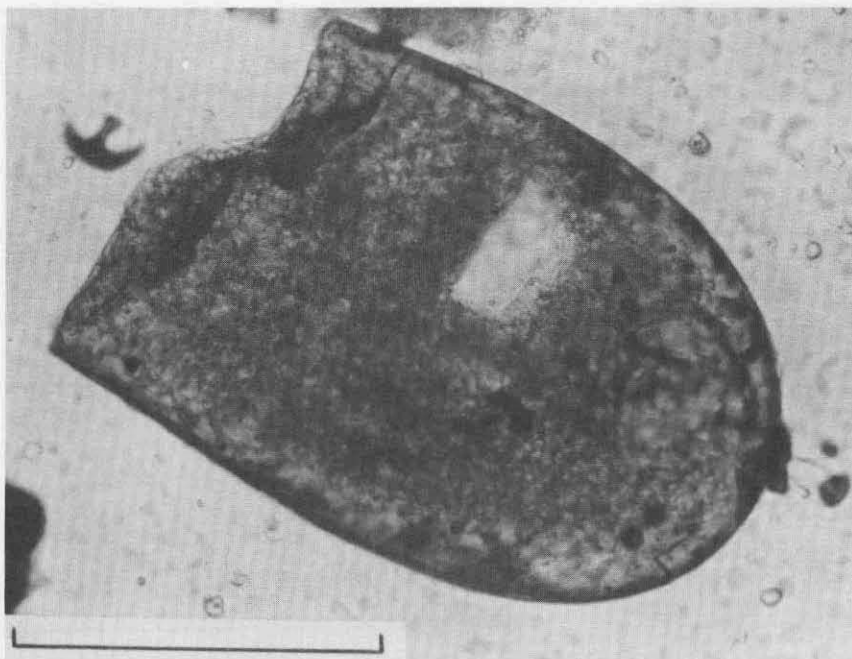


Figure 28A. Broken droplet of light brown glass with included feldspar(?) crystals. Color and texture of the fragment are similar to some light (feldspathic) microbreccias, suggesting formation of the droplet by shock-melting of feldspathic source rocks. Fragment 318,521; plane polarized light; scale bar 0.1 mm.

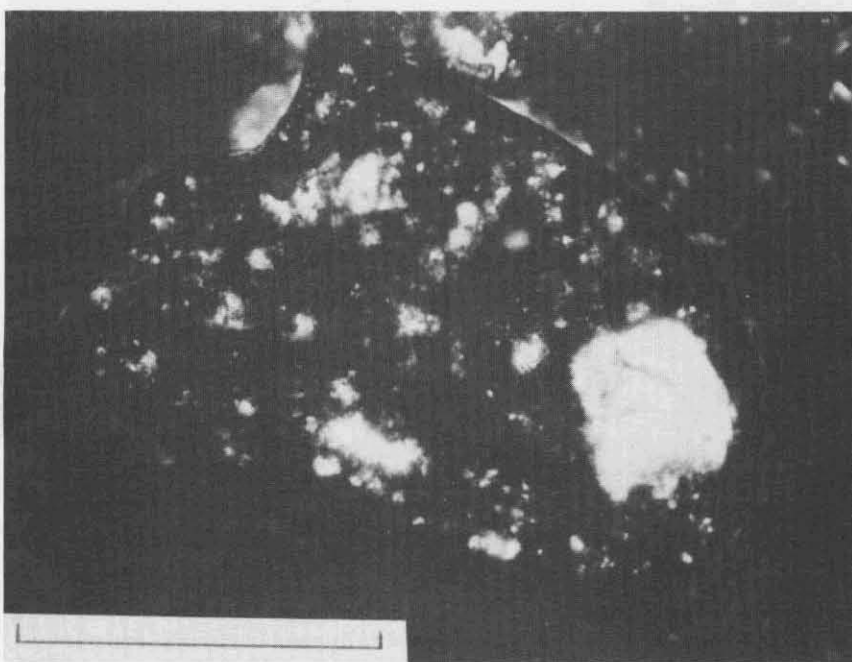


Figure 28B. Same view as Figure 28A; crossed polarizers. Note the numerous small feldspar(?) crystals enclosed in the glass.

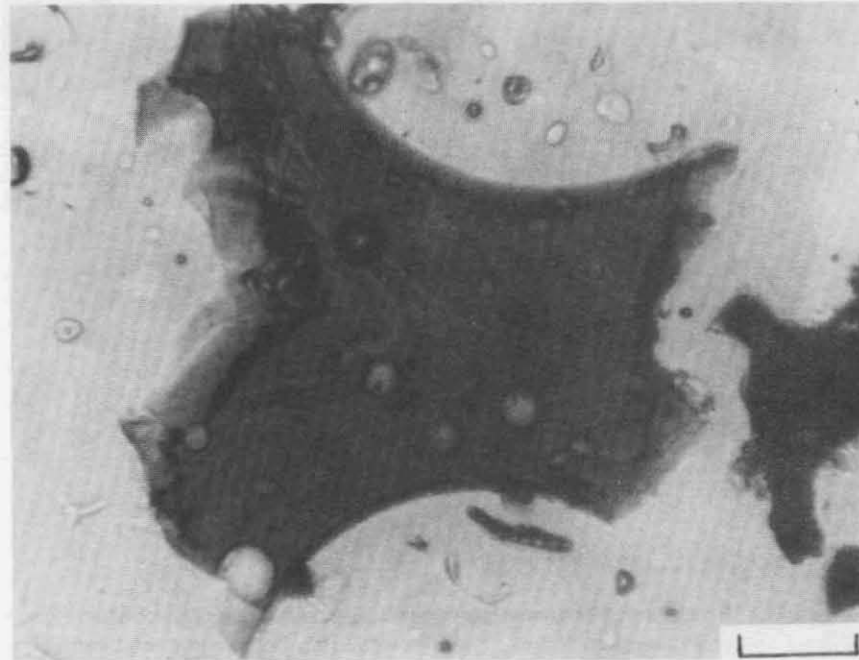


Figure 29. Dense, light green glass fragment with well-developed schlieren of lighter-colored glass forming a contorted flow structure. The curved boundaries at top and bottom suggest that the fragment may have been originally enclosed between two large bubbles in a larger vesicular fragment. Rare Ni-Fe spherules are observed in the glass (very small spherical dark bodies; recognizable in reflected light). Fragment 301,15; plane polarized light; scale bar 0.1 mm.

In quenched fragments that were originally completely glassy, the crystal textures reflect such parameters as the cooling rate and viscosity of the melt and do not provide evidence about the original source of the melt itself. In fragments which lack exotic inclusions, heterogeneous schlieren, or other indicators of impact origin, the crystallization fabrics observed could be produced either by rapid cooling of extruded magma (primary melt) or by rapid quenching of impact-produced glass (secondary; impact melt).

This uncertainty in origin is especially great for a number of fragments which contain fairly large crystals, generally associated with intersertal textures (Figures 39, 41). Two types of such glasses can be distinguished. The more common type is apparently basaltic and has pyroxene as the liquidus phase, accompanied by a high content of fine-grained quench opaques (Figure 39). The second type, which is much less common, contains lathlike crystals of plagioclase which often display skeletal or swallowtail forms and are accompanied by a brown intersertal glass containing fine microlites (pyroxene?). This second type, in which plagioclase is the liquidus phase and opaques are rare, is apparently related to the other feldspathic rocks. It may be either a primary

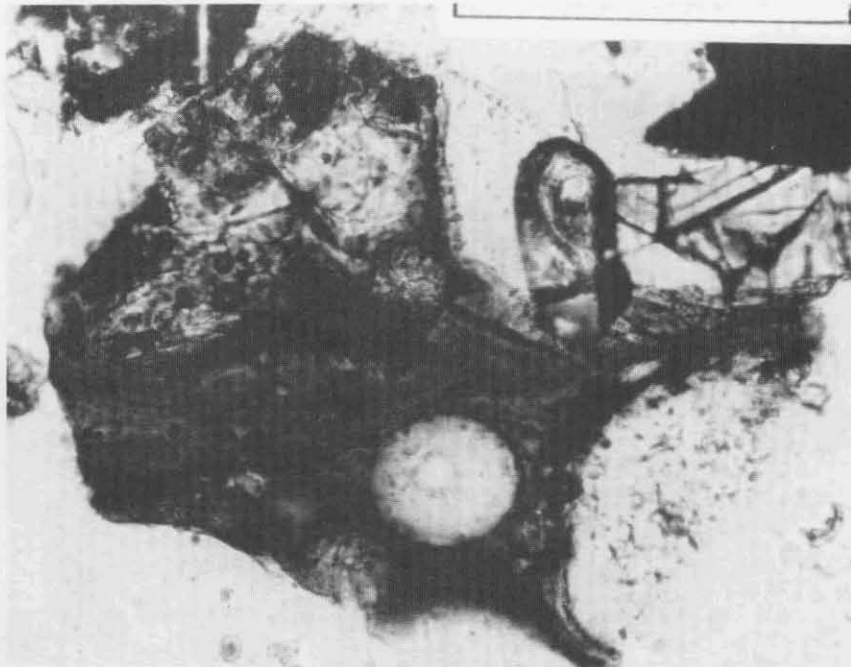


Figure 30. Fragment of brown, heterogeneous, flow-banded glass containing several diverse rock and mineral fragments. The plagioclase-bearing basalt fragment (upper left) shows incipient fusion and assimilation of plagioclase at the contact with the glass; plagioclase is being converted to a clear vesicular glass. The elliptical clear fragment (lower right) is a microcrystalline anorthosite fragment. The pyroxene and opaque grains which occur at upper right are part of an adjacent fragment. Fragment 318,104; plane polarized light; scale bar 0.1 mm.

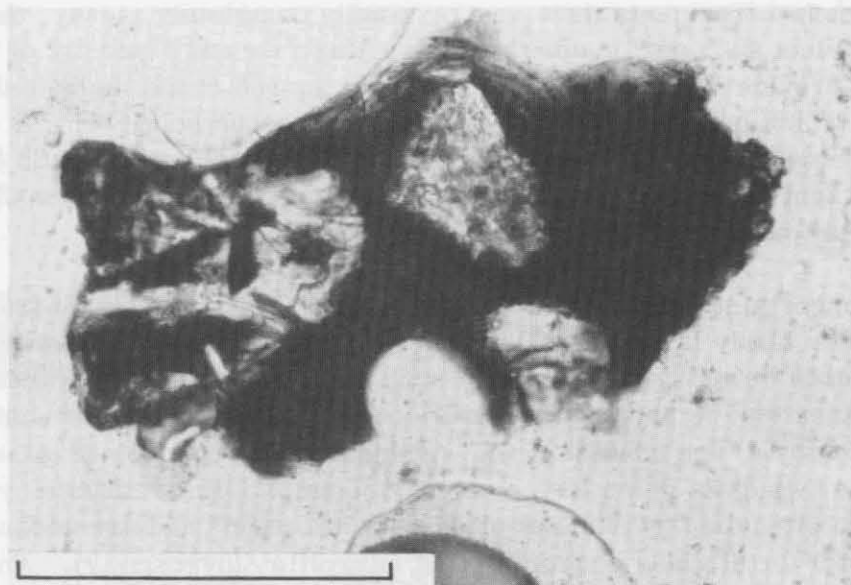


Figure 31. Fragment of dense, dark brown, flow-banded glass containing diverse fragments of ophitic basalt (left), microgranular gabbroic anorthosite (center) and a single crystal of pyroxene or feldspar (lower right). Fragment 318,166; plane polarized light; scale bar 0.08 mm.

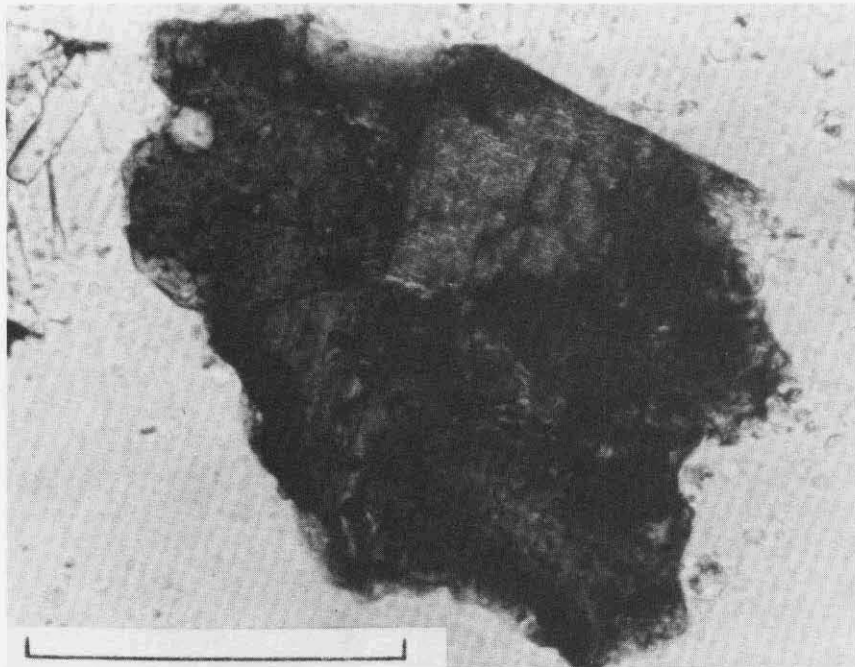


Figure 32. Massive, heterogeneous flow-banded glass with distinct schlieren, enclosing an angular fragment of highly shocked pyroxene(?) which shows strongly mosaic extinction and possible partial isotropization along dark fractures. Fragment 318,37; plane polarized light; scale bar 0.1 mm.

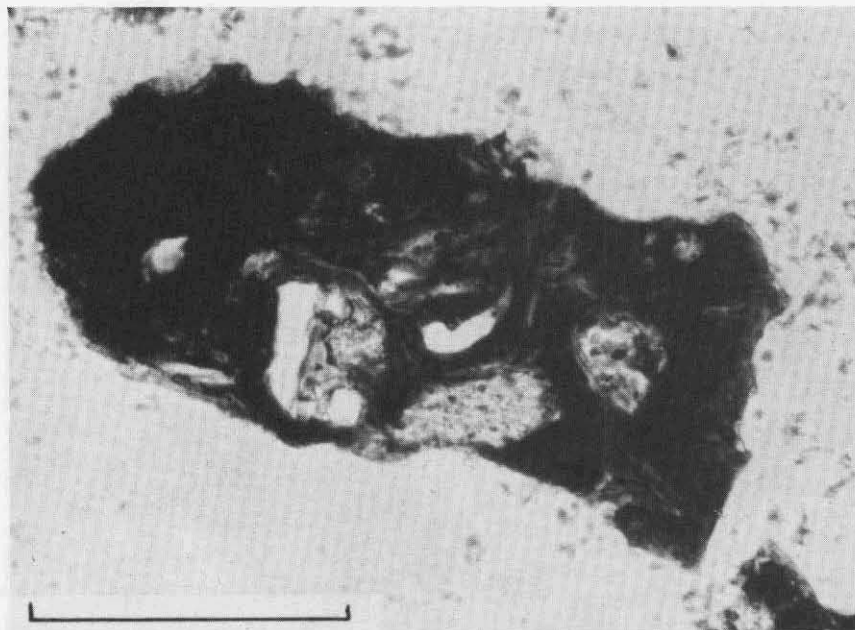


Figure 33. Heterogeneous dark-brown flow-banded glass with partly melted and absorbed inclusions of plagioclase (white, lower center and right) and pyroxene (gray, upper left and upper right). The plagioclase inclusions are partly melted to light greenish and colorless vesicular glasses, forming clear patches and schlieren that are being absorbed into the surrounding glass. Fragment 318,462; plane polarized light; scale bar 0.1 mm.

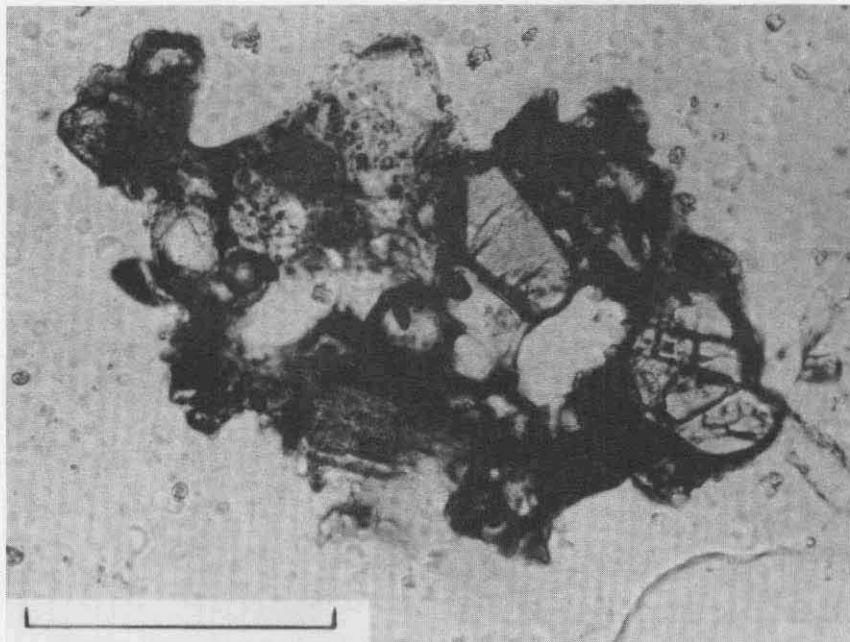


Figure 34. "Glazed aggregate" particle consisting of several mineral fragments cemented by a vesicular matrix of brown glass. Mineral inclusions are pyroxene (gray) and plagioclase (white). The plagioclase grains (upper and left center) are partly converted to colorless vesicular glass. Fragment 318,320; plane polarized light; scale bar 0.1 mm.

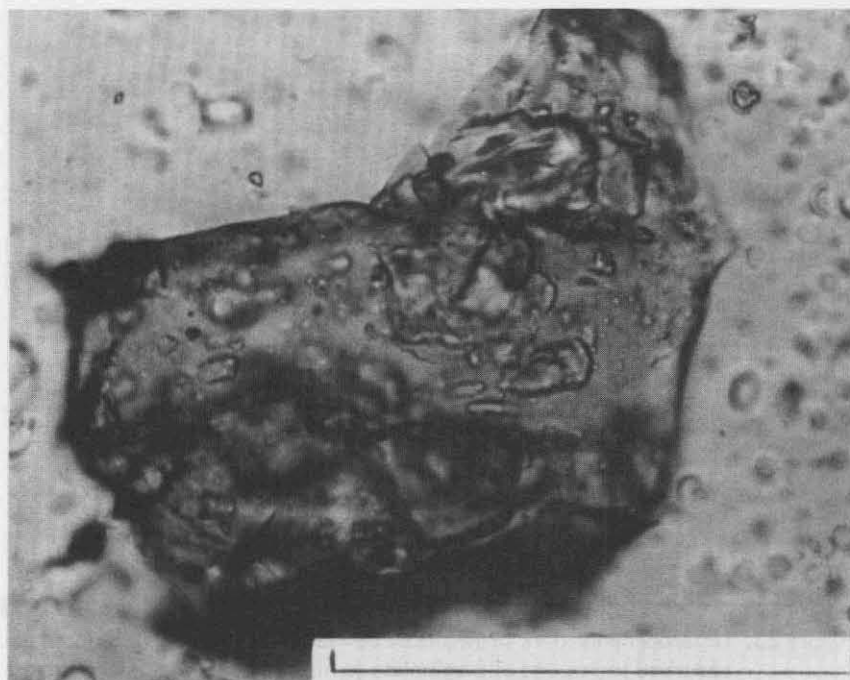


Figure 35. Pale yellow-green glass fragment containing small approximately equant quench(?) crystals (olivine?). Fragment 318,541; plane polarized light; scale bar 0.1 mm.

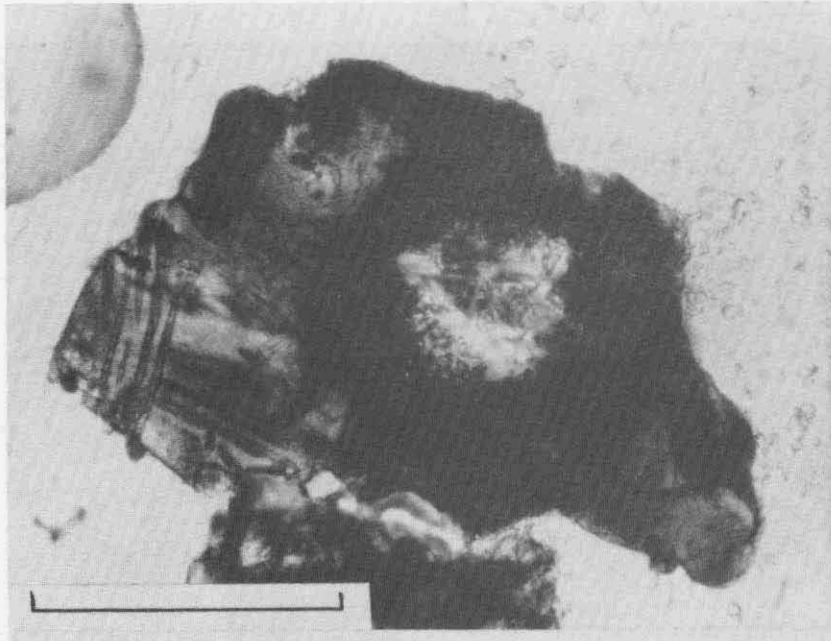


Figure 36. Yellow-brown glass fragment, partly quenched to elongate pyroxene laths (left) and microlites. The large opaque halo surrounds an apparently felsic inclusion and may have been produced by radioactivity in the inclusion. Fragment 318,325; plane polarized light; scale bar 0.1 mm.

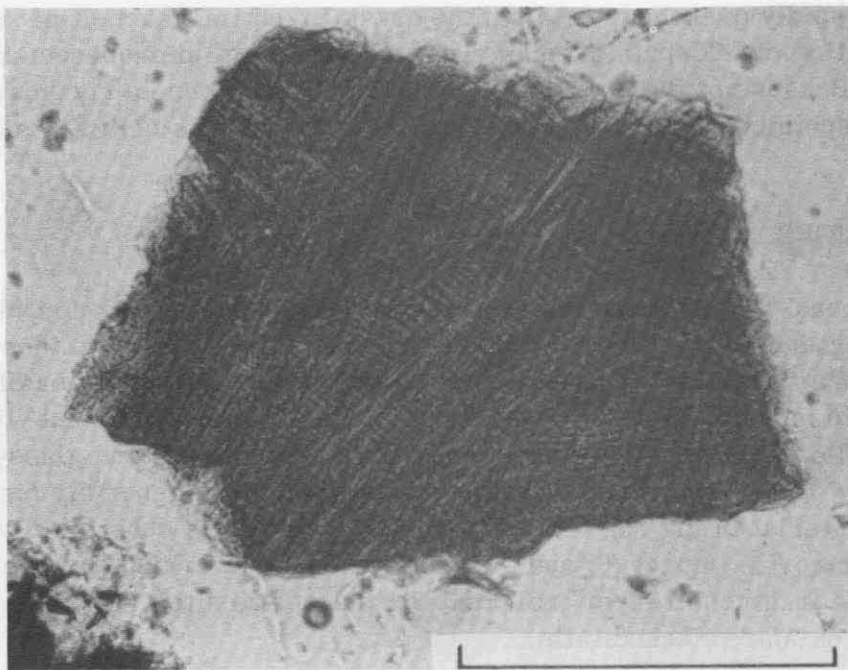


Figure 37. Angular fragment of reddish-brown glass (pyroxene-rich?) containing numerous, diversely oriented quench microlites of a high-relief phase (pyroxene?) in a glass matrix. Fragment 318,73; plane polarized light; scale bar 0.1 mm.

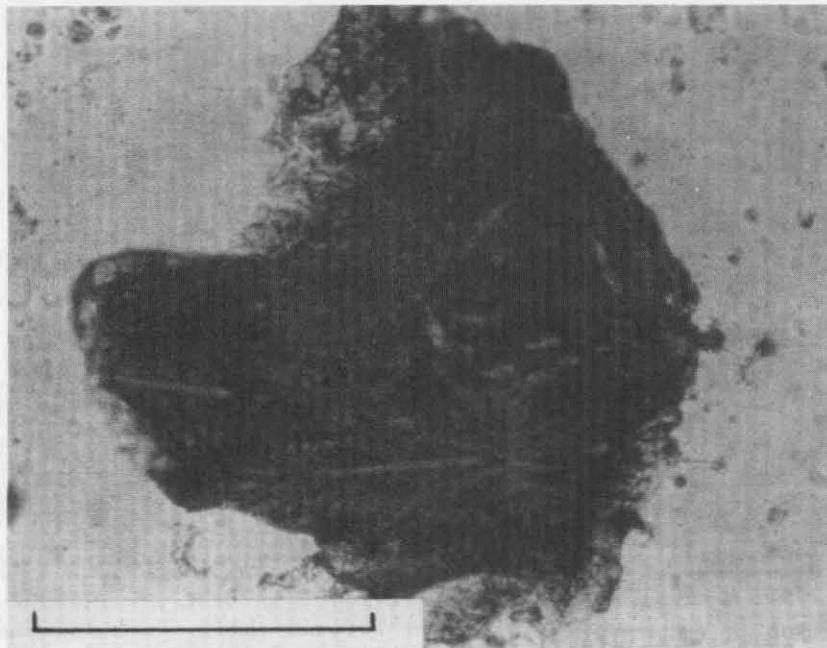


Figure 38. Dark reddish-brown fragment with well-developed quench crystals of pyroxene arranged in parallel and radiating arrays in a matrix of less crystallized glass. Fragment 318,510; plane polarized light; scale bar 0.1 mm.

magma, rapidly quenched, or a partly-crystallized impact melt produced by shock melting of feldspathic rocks similar to the light microbreccias described earlier. Because of the apparent high degree of shock metamorphism in the other feldspathic fragments, the second interpretation is believed more likely.

## CONCLUSIONS

The Luna-16 soil particles exhibit distinctive shock-metamorphic effects, uniquely produced by meteorite impact and virtually identical to those observed in other lunar samples. Distinctive rock and mineral deformation effects are observed in only 1-2 percent of the fragments, a result consistent with studies of the Apollo samples. However, shock-produced glasses and glassy breccias constitute 70-80 percent of the fragments studied. The generally high shock level of material in the regolith on Mare Fecunditatis is consistent with continuous meteorite impact (6) and suggests that the reworking and overturning of the surface fragmental layer indicated for the Apollo sites (1, 5, 11) is also occurring on Mare Fecunditatis.

As in the Apollo samples, two families of source rocks, basaltic and feldspathic, can be recognized in the Luna-16 material. The predominance of

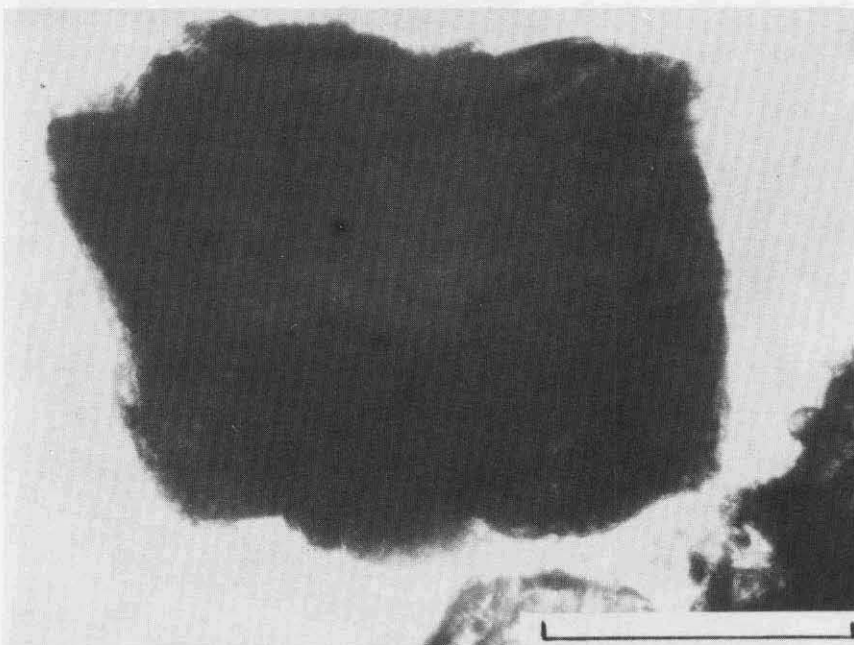


Figure 39A. Dark brownish-black, nearly opaque fragment of glass with extensive development of opaque quench phases. Fragment 318,146; plane polarized light; scale bar 0.1 mm.

Reproduced from  
best available copy.

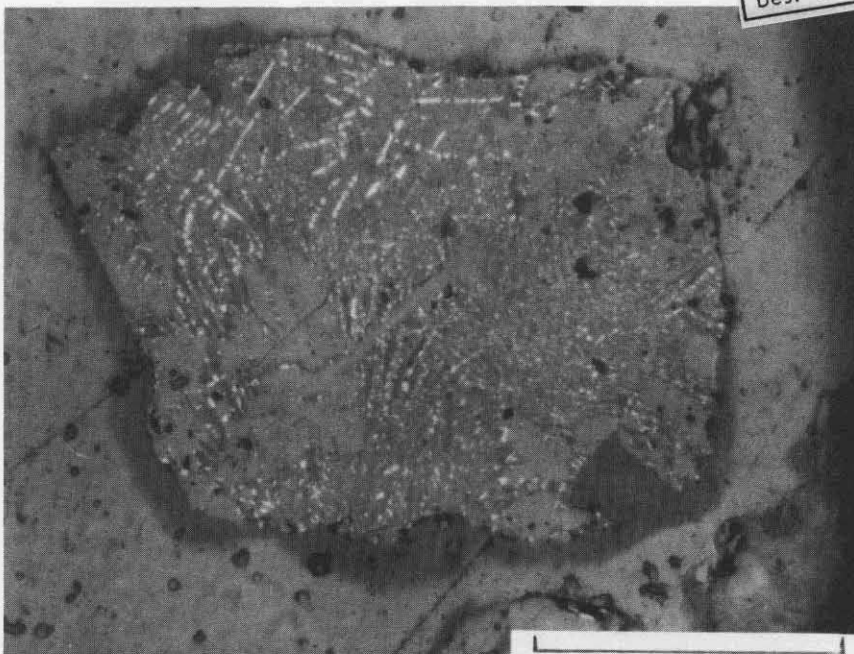


Figure 39B. Same view as Figure 39A; reflected light. The fragment displays well-developed quench textures. Light gray areas are probably pyroxene crystals; darker-gray areas (glass?) contain numerous, small, oriented quench opaque crystals.

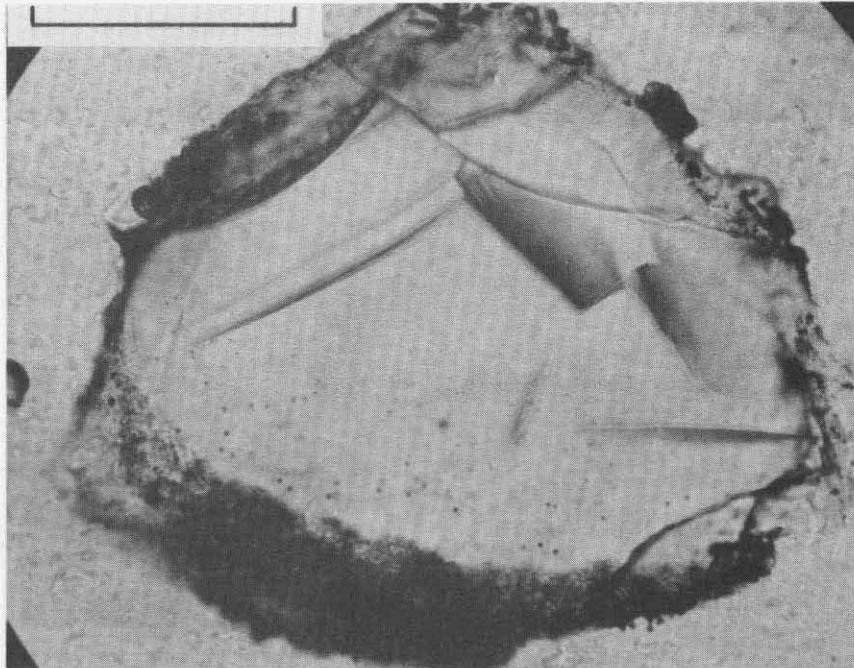


Figure 40A. Partly devitrified fragment of clear, colorless glass with a plagioclase-rich composition. Devitrification to spherulites of fine plagioclase has occurred in a thin marginal rim, often associated with fractures. Fragment 315,175; plane polarized light; scale bar 0.1 mm.

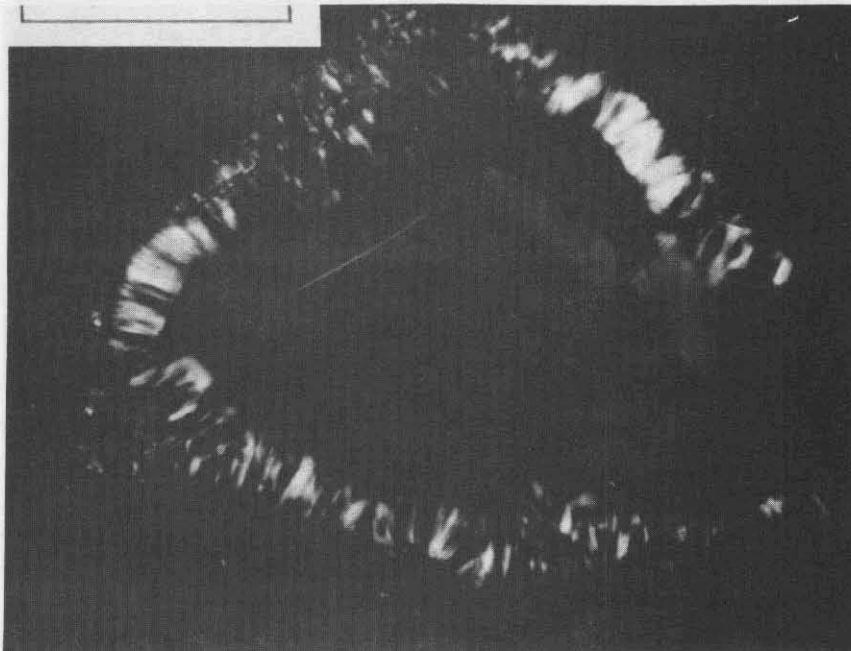
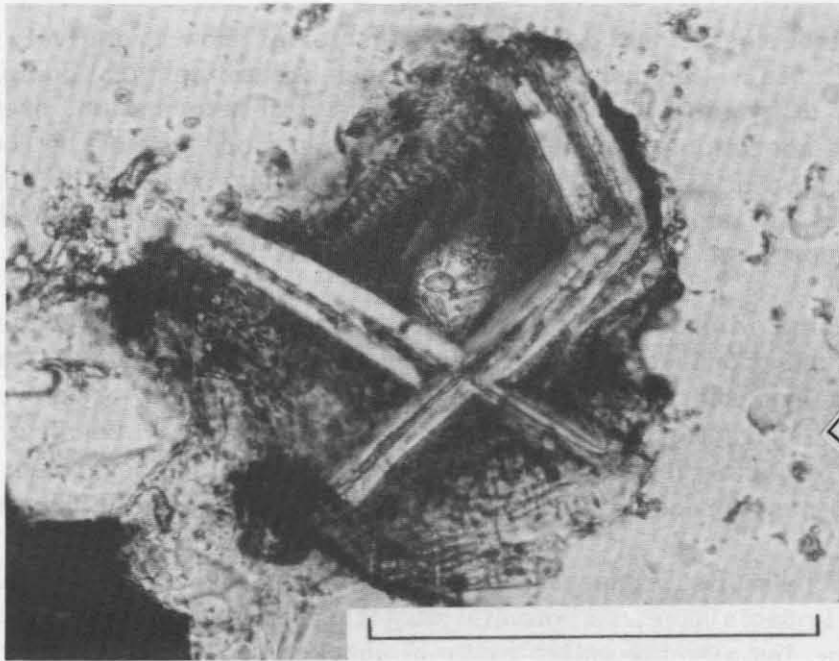


Figure 40B. Same view as Figure 40A; crossed polarizers. A birefringent rim around the fragment is produced by development of plagioclase microlites oriented approximately radially to the surface of the fragment.



Reproduced from  
best available copy.

Figure 41. Glassy inclusion containing large clear skeletal plagioclase laths in a matrix of brownish glass that is partly devitrified to quench micro-lites (pyroxene?). The texture in the fragment suggests rapid cooling and quenching of a melt. It is not clear whether the fragment represents rapidly cooled magmatic rock (a flow margin) (plagioclase microporphyry) or whether the fragment represents quenching of an impact melt formed by fusion of feldspathic source rocks. Fragment 318,377; plane polarized light; scale bar 0.1 mm.

basaltic material and the common occurrence of unshocked basalt fragments indicates that the basaltic rocks are the local bedrock and that Mare Fecunditatis is underlain by basaltic flows which are chemically similar to Apollo 12 material.

The feldspathic rocks (gabbros to anorthosites) are less common, although their abundance is comparable to that observed in Apollo 11 and 12 samples (20, 21). They occur as rare, apparently shocked, rocks and as more common diverse microbreccias. The apparently higher level of shock in the feldspathic rocks is consistent with transport by meteorite impact from source regions outside the Luna-16 landing site. These feldspathic rocks may be highland material (e.g., 6, 20, 21, 24), because the Luna-16 landing site, located near the eastern margin of Mare Fecunditatis (13) might be expected to receive significant amounts of material transported from the nearby highlands. Another possible source of non-mare material would be produced by deeply excavated ejecta from the postmare crater Langrenus about 300 km SE of the landing site.

The source rocks for the Luna-16 soil material show a relatively restricted range of textures and compositions. The much greater textural complexity of the majority of fragments in the soil is the result of deformation, brecciation, melting, and accretion associated with shock metamorphism of the rocks. The flow chart shown in Figure 42 is an attempt to summarize, for the Luna-16 material (and, by implication, for the other lunar soils as well) the effects of shock metamorphism on the presumed source rocks.

Even a single impact event on a uniform source rock will produce a wide range of deformational textures, ranging from simple fracturing to complete fusion, in the shocked material. Single impacts also tend to preserve the original chemical character of the target rock, i. e., impacts on basaltic rocks produce the diverse dark (basaltic) microbreccias, while the occurrence of light (feldspathic) microbreccias implies the existence of feldspathic target rocks.

The products of subsequent or multiple impacts, however, are more complex. Such impacts have, as potential target materials, not only the unaltered source rocks, but also the entire range of shocked rocks and microbreccias produced by earlier impacts. As a result, multiple impacts tend to increase the observed shock level of the soil (6). Multiple impacts also tend to homogenize the regolith by mixing together discrete fragments of originally different chemistry and texture, thus forming composite fragments containing clasts of light microbreccia in dark microbreccia (Figures 9, 12) or cores of light microbreccia surrounded by dark (basaltic?) glass (Figure 13).

In certain cases, as discussed above, the impact-produced melts cannot be distinguished from rapidly quenched magma. In the Luna-16 soil, two types of fragments which reflect quenching of melt produced by either impact or volcanism are the quenched/intersertal basalts (Figures 5, 39) and the plagioclase microporphyry (Figure 41). These relations are indicated by the dashed lines in Figure 42.

The strong evidence for the formation of a fragmental layer at the Luna-16 site by repetitive meteorite impact strengthens the view that this process operates generally over the whole moon. The regolith at the Luna-16 site has apparently been formed by the fragmentation and shock metamorphism of diverse basaltic rocks present on the mare. Additional feldspathic material, apparently more highly shocked, has been introduced into the fragmental layer from an outside source, possibly (though not definitely) from the adjacent highlands or from large craters excavating highland materials. The establishment of such general conclusions about lunar processes by examination of such a small amount of material emphasizes both the usefulness of petrographic methods and the unique character of the shock-metamorphic effects themselves.

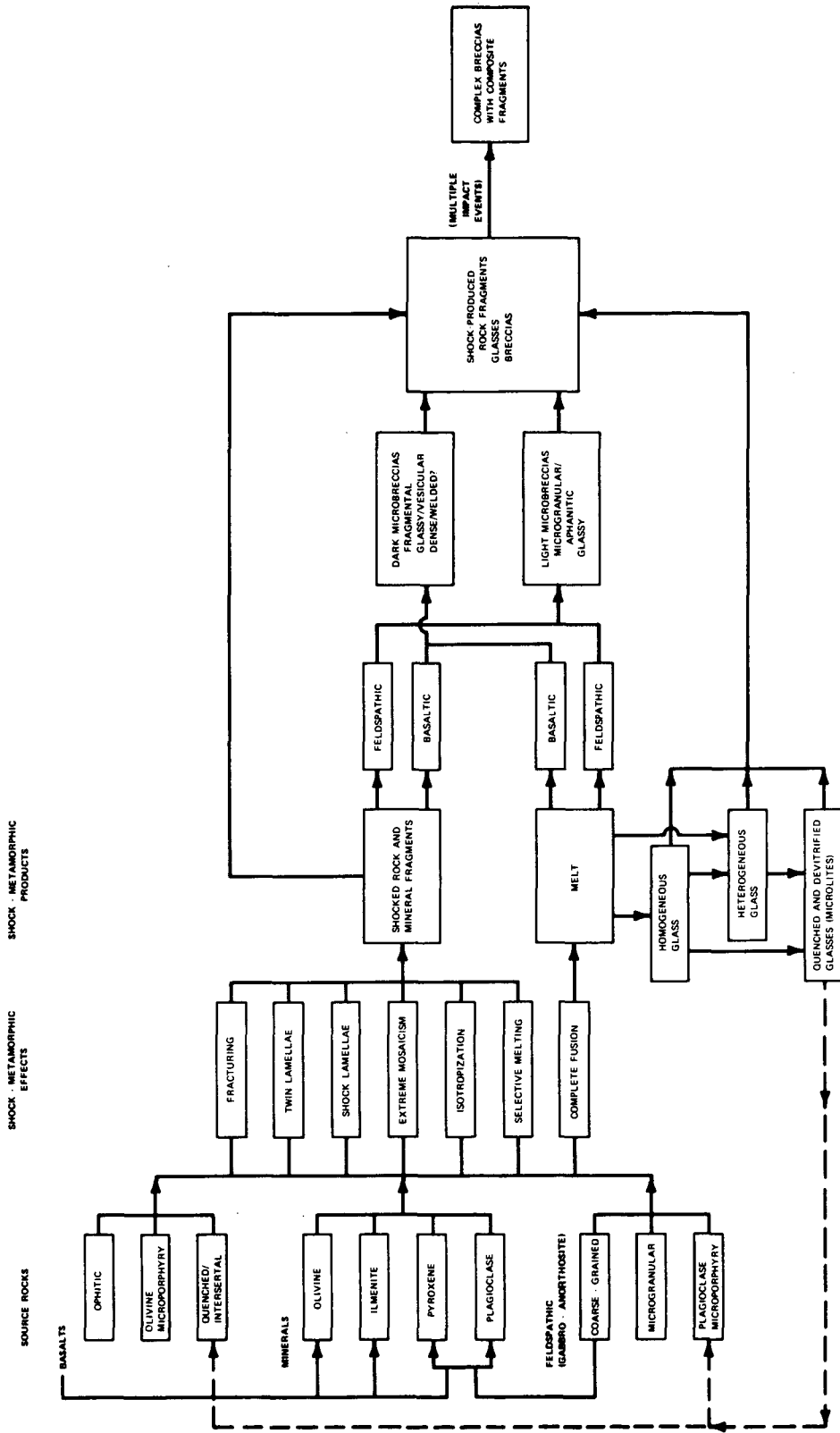


Figure 42. Schematic diagram of shock-metamorphic effects produced in the Luna-16 material by meteorite impacts on the two types of source rocks observed. A single impact produces a wide range of deformational effects but tends to preserve original chemical characteristics. Subsequent multiple impacts affect more diverse target rocks, including previously-produced shock products. Continuing and multiple impacts therefore tend to produce more complex, heterogeneous, and mixed rock types which are common in both light and dark microbreccias. The dashed lines connect textural types produced by quenching of a melt, but whose origin as magma (primary) or as impact melt (secondary) is not clear.

## ACKNOWLEDGEMENTS

I am grateful to J. A. Wood for his advice and encouragement; to M. G. White, for trimming the thin sections down for microprobe work; to A. S. Doan, Jr. and P. Comella, for rapid computer reduction of the microprobe results; to P. D. Lowman, Jr. and W. S. Cameron, for specific suggestions; and to Mary-Hill French, for considerable patience and for a critical review of the manuscript. Special thanks are also due to the many individuals in both the U.S.S.R. and the U.S.A., who contributed toward obtaining these samples and to making possible their exchange for scientific study.

## REFERENCES

1. E. M. Shoemaker, M. H. Hait, G. A. Swann, D. L. Schleicher, G. G. Schaber, R. L. Sutton, D. H. Dahlem, E. N. Goddard, and A. C. Waters, Origin of the lunar regolith at Tranquility Base, in: Proc. Apollo-11 Lunar. Sci. Conf. , vol. 3 (Pergamon Press, 1970) p. 2399.
2. E. C. T. Chao, O. B. James, J. A. Minkin, and J. A. Boreman, Petrology of unshocked crystalline rocks and evidence of impact metamorphism in Apollo 11 returned lunar samples, in: Proc. Apollo-11 Lunar. Sci. Conf. , vol. 1 (Pergamon Press, 1970), p. 287.
3. M. R. Dence, J. A. V. Douglas, A. G. Plant, and R. J. Traill, Petrology, mineralogy, and deformation of Apollo 11 samples, in: Proc. Apollo-11 Lunar Sci. Conf. , vol. 1 (Pergamon Press, 1970), p. 315.
4. W. v. Engelhardt, J. Arndt, W. F. Müller, and D. Stöffler, Shock metamorphism of lunar rocks and the origin of the regolith at the Apollo 11 landing site, in: Proc. Apollo-11 Lunar Sci. Conf. , vol. 1 (Pergamon Press, 1970), p. 363.
5. W. Quaide and T. Bunch, Impact metamorphism of lunar surface materials, in: Proc. Apollo-11 Lunar Sci. Conf. , vol. 1 (Pergamon Press, 1970), p. 711.
6. N. M. Short, The nature of the moon's surface: evidence from shock metamorphism in Apollo 11 and 12 samples, Icarus 13 (1970), p. 383.
7. E. C. T. Chao, J. A. Borman, J. A. Minkin, O. B. James, and G. A. Desborough, Lunar glasses of impact origin: physical and chemical characteristics, J. Geophys. Res. 75 (1970) p. 7445.
8. E. C. T. Chao, J. A. Boreman, and G. A. Desborough, The petrology of unshocked and shocked Apollo 11 and Apollo 12 microbreccias, in: Proc. 2nd Lunar Sci. Conf. , vol. 1 (M. I. T. Press, 1971), p. 797.
9. C. B. Sclar, Shock-induced features of Apollo 12 microbreccias, in: Proc. 2nd Lunar Sci. Conf. , vol. 1 (M. I. T. Press, 1971), p. 817.
10. W. v. Engelhardt, J. Arndt, W. F. Müller, and D. Stöffler, Shock metamorphism and origin of the regolith and breccias at the Apollo 11 and Apollo 12 landing sites, in: Proc. 2nd Lunar Sci. Conf. , vol. 1 (M. I. T. Press, 1971), p. 833.

11. W. Quaide, V. Oberbeck, T. Bunch, and G. Polkowski, Investigations of the natural history of the regolith at the Apollo 12 site, in: Proc. 2nd Lunar Sci. Conf. , vol. 1 (M. I. T. Press, 1971), p. 701.
12. LSPEP (Lunar Sample Preliminary Examination Team), Preliminary examination of lunar samples from Apollo 14, Science 173 (1971), p. 681.
13. A. P. Vinogradov, Preliminary data on lunar ground brought to Earth by automatic probe, "Luna-16," in: Proc. 2nd Lunar Sci. Conf. , vol. 1 (M. I. T. Press, 1971), p. 1.
14. B. M. French, L. S. Walter, K. F. J. Heinrich, A. S. Doan, P. D. Lowman, and I. Adler, Compositions of major and minor minerals in five Apollo 12 crystalline rocks, NASA Spec. Public. (SP), in press.
15. A. J. Doan and R. L. Schmadebeck, A new concise treatment of X-ray microprobe data after Bence and Albee, NASA Goddard Space Flight Center, X-document, in press.
16. S. O. Agrell, J. H. Scoon, I. D. Muir, J. V. P. Long, J. D. C. McConnell, and A. Peckett, Observations on the chemistry, mineralogy and petrology of some Apollo 11 lunar samples, in: Proc. Apollo-11 Lunar Sci. Conf. , vol. 1 (Pergamon Press, 1970), p. 93.
17. M. B. Duke, C. C. Woo, G. A. Sellers, M. L. Bird, and R. B. Finkleman, Genesis of lunar soil at Tranquillity Base, in Proc. Apollo-11 Lunar Sci. Conf. , vol. 1 (Pergamon Press, 1970), p. 347.
18. D. S. McKay, W. R. Greenwood, and D. A. Morrison, Origin of small lunar particles and breccia from Apollo 11 site, in: Proc. Apollo-11 Lunar Sci. Conf. , vol. 1 (Pergamon Press, 1970), p. 673.
19. E. A. King, M. F. Carman, and J. C. Butler, Mineralogy and petrology of coarse particulate material from the lunar surface at Tranquillity Base, in: Proc. Apollo-11 Lunar Sci. Conf. , vol. 1 (Pergamon Press, 1970), p. 599.
20. J. A. Wood, Petrology of the lunar soil and geophysical implications, J. Geophys. Res. 75 (1970), p. 6497.
21. U. B. Marvin, J. A. Wood, G. T. Taylor, J. B. Reid, B. N. Powell, J. S. Dickey, and J. F. Bower, Relative proportions and probable sources of rock fragments in the Apollo 12 soil samples, in: Proc. 2nd Lunar Sci. Conf. , vol. 1 (M. I. T. Press, 1971), p. 679.

22. C. Meyer, R. Brett, N. J. Hubbard, D. A. Morrison, D. S. McKay, F. K. Aitken, H. Takeda, and E. Schonfeld, Mineralogy, chemistry, and origin of the KREEP component in soil samples from the Ocean of Storms, in: Proc. 2nd Lunar Sci. Conf., vol. 1 (M. I. T. Press, 1971), p. 393.
23. A. T. Anderson and J. V. Smith, Nature, occurrence, and exotic origin of "gray mottled" (Luny Rock) basalts in Apollo 12 soils and breccias, in: Proc. 2nd Lunar Sci. Conf., vol. 1 (M. I. T. Press, 1971), p. 431.
24. J. A. Wood, J. B. Reid, G. J. Taylor, and U. B. Marvin, Petrological character of the Luna 16 sample from Mare Fecunditatis, Meteoritics 6 (1971), p. 181.
25. N. L. Carter, I. S. Leung, H. G. Ave'Lallemant, and L. A. Fernandez, Growth and deformational structures in silicates from Mare Tranquillitatis, in: Proc. Apollo-11 Lunar Sci. Conf., vol. 1 (Pergamon Press, 1970), p. 267.
26. U. Hornemann, and W. F. Müller, Shock-induced deformation twins in clinopyroxene, Neues Jahrb. Mineral. Mh. 6 (1971), p. 247.
27. S. E. Haggerty, F. R. Boyd, P. M. Bell, L. W. Finger, and W. B. Bryan, Opaque minerals and olivine in lavas and breccias from Mare Tranquillitatis, in: Proc. Apollo-11 Lunar Sci. Conf., vol. 1 (Pergamon Press, 1970), p. 513.